BioSystems 164 (2018) 199–216

Contents lists available at ScienceDirect

BioSystems

journal homepage: www.elsevier.com/locate/biosystems

Genetic coding algorithm for sense and antisense peptide interactions

Nikola Štambuk[a,*], Paško Konjevoda[b], Petra Turčić[c], Katalin Kövér[d], Renata Novak Kujundžić[b], Zoran Manojlović[e], Mario Gabričević[f]

[a] Center for Nuclear Magnetic Resonance, Ruđer Bošković Institute, Bijenička cesta 54, HR-10000 Zagreb, Croatia
[b] Laboratory for Epigenomics, Division of Molecular Medicine, Ruđer Bošković Institute, Bijenička cesta 54, HR-10000 Zagreb, Croatia
[c] Department of Pharmacology, Faculty of Pharmacy and Biochemistry, University of Zagreb, Domagojeva 2, HR-10000 Zagreb, Croatia
[d] University of Debrecen, Department of Inorganic and Analytical Chemistry, H-4010 Debrecen P.O. Box 21, Hungary
[e] Croatian Institute for Toxicology and Anti-doping, Borongajska 83g, HR-10000 Zagreb, Croatia
[f] Department of General and Inorganic Chemistry, Faculty of Pharmacy and Biochemistry, University of Zagreb, Ante Kovačića 1, HR-10000 Zagreb, Croatia

ARTICLE INFO

Article history:
Received 10 July 2017
Received in revised form 13 October 2017
Accepted 16 October 2017
Available online 28 October 2017

Keywords:
Genetic code
Complementary sequence
Peptide interaction
Hydrophobic
Lipophilic
mRNA
tRNA

ABSTRACT

Sense and antisense peptides, i.e. peptides specified by complementary DNA and RNA sequences, interact with increased probability. Biro, Blalock, Mekler, Root-Bernstein and Siemion investigated the recognition rules of peptide—peptide interaction based on the complementary coding of DNA and RNA sequences in 3′ → 5′ and 5′ → 3′ directions. After more than three decades of theoretical and experimental investigations, the efficiency of this approach to predict peptide—peptide binding has been experimentally verified for more than 50 ligand—receptor systems, and represents a promising field of research. The natural genetic coding algorithm for sense and antisense peptide interactions combines following elements: of amino acid physico-chemical properties, stereochemical interaction, and bidirectional transcription. The interplay of these factors influences the specificity of sense—antisense peptide interactions, and affects the selection and evolution of peptide ligand—receptor systems. Complementary *mRNA codon—tRNA anticodon complexes*, and recently discovered Carter-Wolfenden *tRNA acceptor-stem code*, provide the basis for the rational modeling of peptide interactions based on their hydrophobic and lipophilic amino acid physico-chemical properties. It is shown that the interactions of complementary amino acid pairs according to the hydrophobic and lipophilic properties strongly depend on the central (second) *purine base* of the mRNA codon and its *pyrimidine* complement of the tRNA anticodon. This enables the development of new algorithms for the analysis of structure, function and evolution of protein and nucleotide sequences that take into account the residue's tendency to leave water and enter a nonpolar condensed phase considering its mass, size and accessible surface area. The practical applications of the sense—antisense peptide modeling are illustrated using different interaction assay types based on: microscale thermophoresis (MST), tryptophan fluorescence spectroscopy (TFS), nuclear magnetic resonance spectroscopy (NMR), and magnetic particles enzyme immunoassay (MPEIA). Various binding events and circumstances were considered, e.g., in situations with—short antisense peptide ligand (MST), L- and D-enantiomer acceptors (TFS), in low affinity conditions (NMR), and with more than one antisense peptide targeting hormone (MPEIA).

1. Introduction

The standard genetic code defines rules for the transcription of biological DNA and RNA information, and related protein synthesis, namely translation rules. It is often described as a translation table by which nucleic acid sequence information is interpreted as polypeptide (Carter and Wolfenden, 2016). The natural property of the genetic code is the "complementarity principle", defined by the physicochemical nucleotide interaction, i.e. pairing, of uracil (U) or thymine (T) with adenine (A), and cytosine (C) with guanine (G) (Table 1A).

A large body of theoretical and experimental evidence over the last three decades supports the thesis that peptides specified by the complementary DNA and RNA sequences, i.e. sense and antisense peptides, interact with increased probability (Root-Bernstein, 2015; Root-Bernstein, 2005; Biro, 2007; Siemion et al., 2004; Miller, 2015; Blalock, 1995; Štambuk et al., 2014). The idea of

* Corresponding author.
E-mail addresses: stambuk@irb.hr (N. Štambuk), pkonjev@irb.hr (P. Konjevoda), pturcic@pharma.hr (P. Turčić), kover@tigris.unideb.hu (K. Kövér), rnovak@irb.hr (R.N. Kujundžić), zoran.manojlovic@antidoping-hzta.hr (Z. Manojlović), mariog@pharma.hr (M. Gabričević).

https://doi.org/10.1016/j.biosystems.2017.10.009

Table 1
(**A**) Standard genetic code Table. Sixty-four 3-letter codons specifiy 20 amino acids and 3 stop codons for the protein synthesis. (**B**) The number of complementary (sense – antisense) amino acid pairs depends on the direction of translation (3′ → 5′ = left → right or 5′ → 3′ = right → left).

A

First (5′) letter	Second letter				Third (3′) letter
	U	C	A	G	
U	F	S	Y	C	U
	F	S	Y	C	C
	L	S	stop	stop	A
	L	S	stop	W	G
C	L	P	H	R	U
	L	P	H	R	C
	L	P	Q	R	A
	L	P	Q	R	G
A	I	T	N	S	U
	I	T	N	S	C
	I	T	K	R	A
	M	T	K	R	G
G	V	A	D	G	U
	V	A	D	G	C
	V	A	E	G	A
	V	A	E	G	G

B

Amino acid	Antisense 3′ → 5′	Antisense 5′ → 3′
F	K	K, E
L	D, E, N	E, Q, K
I	Y	N, D, Y
M	Y	H
V	H, Q	H, D, N, Y
S	S, R	G, R, T, A
P	G	G, W, R
T	W, C	G, S, C, R
A	R	R, G, S, C
Y	M, I	I, V
H	V	V, M
Q	V	L
N	L	I, V
K	F	F, L
D	L	I, V
E	L	L, F
C	T	T, A
W	T	P
R	A, S	A, S, P, T
G	P	P, S, T, A

sense and antisense peptide binding, mediated by specific through-space amino acid paired interactions, was first proposed by Mekler (Biro, 2007; Tropsha et al., 1992; Mekler, 1970; Mekler and Idlis, 1981). Biro, Blalock, Root-Bernstein and Siemion investigated different aspects of peptide—peptide interaction based on the coding of antisense DNA and RNA sequences in 3′ → 5′ and 5′ → 3′ directions (Table 1B). Critical examination of the concept has confirmed the relevance and applicability of antisense peptides to *in vitro* and *in vivo* research (Root-Bernstein, 2015; Root-Bernstein, 2005; Biro, 2007; Siemion et al., 2004; Miller, 2015; Blalock, 1995; Štambuk et al., 2014).

Until recently, most discussions related to the physico-chemical properties of antisense peptides relied on the concept of classic hydropathy (Miller, 2015; Blalock, 1995) based on the fact that the second base of the messenger RNA (mRNA) codon specifies amino acid hydropathy as an important factor regarding protein interactions. The hydropathy index of an amino acid was proposed in 1982 by Jack Kyte and Russell F. Doolittle (Kyte and Doolittle, 1982) as a number representing the hydrophobic or hydrophilic properties of amino acid side chains.

In this study we investigate sense-antisense peptide relationships using a new transfer RNA (tRNA) acceptor-stem code, introduced by Carter and Wolfenden (Carter and Wolfenden, 2015). This acceptor-stem code, related to amino acid size and lipophilicity, is distinct from the code in the anticodon that is based on amino acid hydrophobicity or hydrophilicity, and preserves key properties of stereochemically-encoded peptides.

2. Results and discussion

2.1. Antisense peptides and complementary nucleotide coding

The purposeful design of specific bioactive complements is related to the theory that antisense peptides or proteins bind with high affinity to each other (Root-Bernstein, 2015; Root-Bernstein, 2005; Biro, 2007; Siemion et al., 2004; Miller, 2015; Blalock, 1995; Štambuk et al., 2014). According to Siemion et al. there are three main hypotheses concerning the interaction of sense—antisense peptides based on complementary coding principles (Siemion et al., 2004):

1. the Root-Bernstein approach to the interaction of complementary peptides, which is based on the stereochemical interaction of sense—antisense amino acids coded by anticodons read in parallel with the coding DNA strand (3′ → 5′ translation).
2. the Mekler-Blalock antisense hypothesis, which is based on the hydropathic complementarity principle of the sense—antisense interaction that is independent of the direction of triplet reading (5′ → 3′/3′ → 5′), since the central base of the coding triplet specifies the hydropathy of the amino acid.
3. the Siemion hypothesis of sense—antisense peptide interaction, which is based on the periodicity of the genetic code, i.e. *the Siemion one-step mutation ring of the code*, that is related to: a) *the Argyle amino acid similarity ring* (residue replacement during evolution), b) *the Pieber-Tohác amino acid ring*, i.e. codon replacement probability matrix, and c) the Chou-Fasman conformational parameters and amino acid compositional frequencies in proteins. The resulting sense—antisense amino acid pairs are in most cases similar to 3′ → 5′ translation according to Root-Bernstein.

2.1.1. Rules and patterns of complementary peptide coding

The algorithms for the antisense peptide design based on complementary peptide binding in the 3′ → 5′ and 5′ → 3′ translation direction were introduced in the 1980s by Root-Bernstein (Root-Bernstein, 2015; Root-Bernstein, 2005; Root-Bernstein, 1982) and Blalock et al. (Blalock, 1995; Blalock and Bost, 1986; Zull and Smith, 1990), and their efficiency has been experimentally verified for more than 50 ligand—receptor systems (Root-Bernstein, 2015; Root-Bernstein, 2005; Biro, 2007; Siemion et al., 2004; Miller, 2015; Blalock, 1995; Štambuk et al., 2014).

Simple transformations of complementary (sense—antisense) peptide coding in both directions (*left* → *right* and *vice versa*) define pivotal aspects of the natural code presented in Table 1:

1. two of the basic types of sense—antisense amino acid hydropathy patterns (neutral-neutral, nonpolar-polar) are *symmetric*, i.e. of identical pattern type, with respect to *left* → *right* and *right* → *left* translation of the coding table (Fig. 1);
2. two of the basic types of sense – antisense amino acid hydropathy patterns are *assymetric—chiral*, i.e. of different pattern number, with respect to *left* → *right* and *right* → *left* translation of the coding table (Fig. 1).

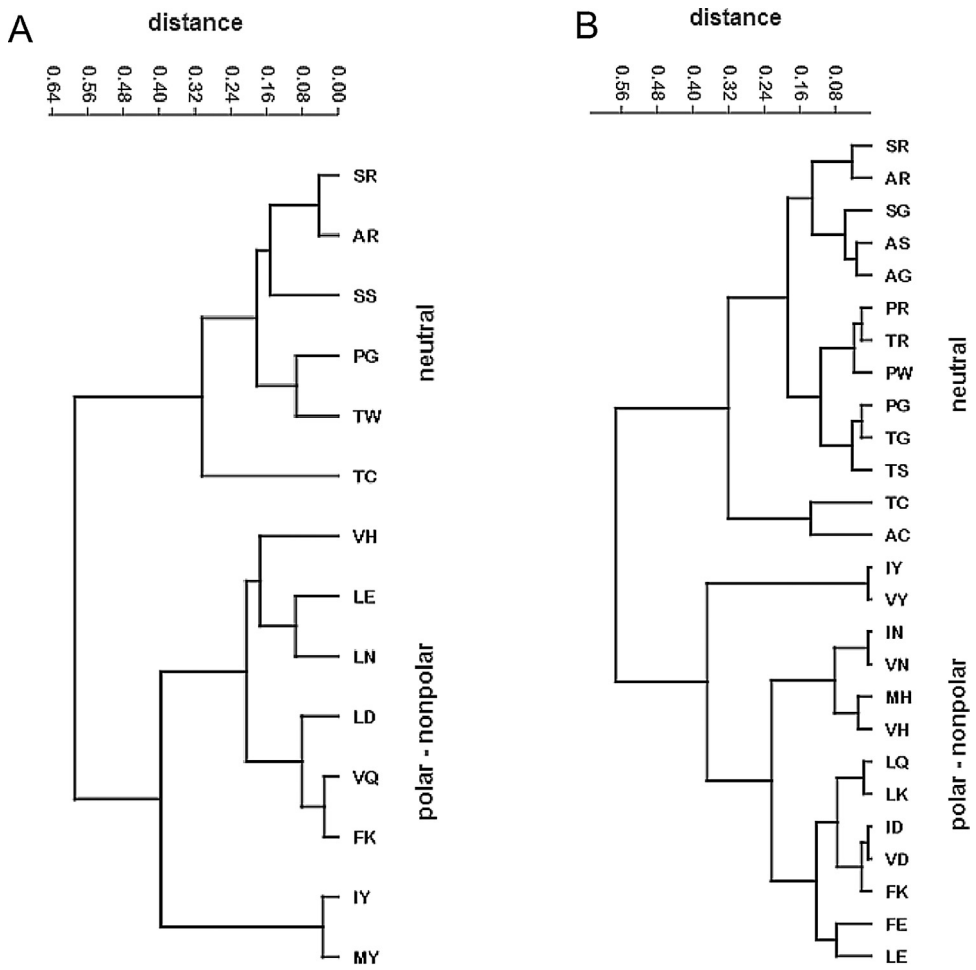

Fig. 1. Hydrophobicity PRIFT values of the complementary amino acid pairs in Table 1B form two distinct clusters composed of polar-nonpolar and neutral residues. (**A**) Complementary (sense—antisense) pairs of the genetic code translated in $3' \rightarrow 5'$ direction, r = 0.86; (**B**) Complementary (sense—antisense) pairs of the genetic code translated in $5' \rightarrow 3'$ direction, r = 0.87. Paired group algorithm, Gower similarity index (PAST software, version 3.16).

The complementary amino acid pairs presented in Table 1B differ in the number of patterns, e.g., 27 pairs are derived by $3' \rightarrow 5'$ translation (13×2 and one SS pair) and 52 by $5' \rightarrow 3'$ one (26×2). Consequently, for antisense peptides the total number of complementary amino acid pairs (N) translated in a $3' \rightarrow 5'$ direction is approximately the square root of the number of complementary amino acid pairs translated in $5' \rightarrow 3'$ direction, i.e. $N_{3' \rightarrow 5'} \approx \sqrt{N_{5' \rightarrow 3'}}$ (Table 1B). The latter result arises from the fact that $5' \rightarrow 3'$ complementary transformation is comprised of 16 groups of codons, while $3' \rightarrow 5'$ complementary transformation is comprised of 4 groups, as shown in Table 1A and B (Štambuk et al., 2016a; Štambuk and Konjevoda, 2016). In addition to the huge difference in the number of antisense peptides according to the direction of translation, the problem of amino acid complementarity is still unresolved with respect to the factors of protein folding and protein—protein complexation. Root-Bernstein claims that the antisense approach only applies to peptides that lack significant secondary and tertiary conformation, which is often valid for the structures of <20 amino acids, while Blalock maintains that the antisense approach applies to entire proteins and that complementary proteins fold into complementary shapes (Root-Bernstein, 2005). The experimental observation that affinity of sense and antisense peptides is tolerant to significant amino acid substitutions was explained by two factors (Tropsha et al., 1992): 1. the conservative substitution of sense-antisense peptide pairing arising from the genetic code structure, and 2. the fact that "dependence of binding on multiple contacts may lessen the impact of a non-conservative amino acid substitution" (Tropsha et al., 1992).

Antisense peptide design based on $3' \rightarrow 5'$ sequence translation leads to significantly fewer antisense peptide structures being obtained, and consequently seems to be a plausible alternative in situations when the screening of bioactive antisense ligands is considered (Root-Bernstein, 2005; Štambuk et al., 2014).

2.2. Hydrophobicity and residue contact potential are related to sense—antisense peptide coding

The hydrophobicity values of individual amino acids affects the characteristic periodicity of the amphipatic structures of proteins (Cornette et al., 1987), and influences secondary and tertiary protein structure. Cornette et al. (Cornette et al., 1987) compared 38 published hydrophobicity scales and derived an optimum normalized scale (PRIFT) for associating amphipathic secondary structure in a protein molecule with the sequence of hydrophobicity values of its residues. PRIFT denotes the maximized amphipathic index of the Fourier transform (FT) composite power spectrum for the primary (PRI) set of helices (Cornette et al., 1987), and represents a useful tool for different bioinformatic applications concerning protein structure-function modeling (Štambuk and Konjevoda, 2017a; Štambuk and Konjevoda, 2017b). Fig. 1**A** and **B** show that the PRIFT scale has a high correlation with the complementary coding of sense – antisense peptide pairs that arise from translation in both directions. Considering the amino acid "hydrophobic character"

of PRIFT (Cornette et al., 1987), the extraction of coding patterns for sense—antisense pairs in both translation directions implies that the complementary coding algorithm for sense—antisense peptide interactions represents a general rule based on residue hydrophobic potential. The reason for this may be the fact that in addition to predicting α-amphipathicity the method of Cornette et al. is highly successful in identifying β-amphipathicity (Cornette et al., 1987), and in distinguishing exterior from interior residues in proteins—known to be strongly correlated to the pairing preferences in complementary amino acid pairs (Siemion et al., 2004). In 1992, Tropsha et al. used the term "amphipathic recognition" for a hydrophilic-hydrophobic mechanism of sense-antisense peptide binding, and noted that several observations support the proposed mechanism of "amphipathic complementarity" (Tropsha et al., 1992).

The results presented in Fig. 1 are supported by Miyazawa-Jernigan residue–residue contact potentials (Štambuk et al., 2016a; Štambuk and Konjevoda, 2016; Miyazawa and Jernigan, 1999). This model additionally supports the recognition rules of sense—antisense peptide interaction, and is widely used as a knowledge-based potential for globular proteins being derived using the quasi-chemical approximation from large databases of proteins with known 3D structures. The critical distance for efficient modeling with the Miyazawa-Jernigan method (<6.5 Å) satisfies the recommended criteria for an accurate protein—protein interaction algorithms, which include different bonding types (e.g., ionic or electrostatic bonds, hydrogen bonds, van der Waals and hydphobic interactions, or multiple bonding types) (Štambuk et al., 2016a; Miyazawa and Jernigan, 1999; Miyazawa and Jernigan, 1985; Mihel et al., 2008). Calculations and clustering procedures (Štambuk et al., 2016a; Štambuk and Konjevoda, 2016) confirmed that complementary amino acid interactions are equally well explained by Miyazawa-Jernigan interaction energies among residues that consist of: contact energies only (method A), paired contact energies (method B), repulsive packing energies (method C), and secondary structure energies (method D). This implies that the result was not dependent on the characteristics of the equilibrium distributions of contacts in observed protein structures (Štambuk et al., 2016a; Miyazawa and Jernigan, 1999), that is, the result relating to amino acid complementarity patterns represents a general rule within a critical distance of within 6.5 Å (Štambuk et al., 2016a). Agglomerative hierarchical clustering (HAC) on results from a principal component analysis (PCA) also confirms that PRIFT and Myazawa D parameters have identical information content, i.e. they contribute equally to the explanation of variance between data points (Le and Worch, 2014).

Table 2 shows that the PRIFT results correlate strongly with those produced using the method of Manavalan-Ponnuswamy (Manavalan and Ponnuswamy, 1978). The difference between Miyazawa-Jernigan and Manavalan-Ponnuswamy methods is that the former uses side chain contact positions, and contacts among residues and effective solvent molecules within 6.5 Å distance, while the latter uses a sphere of 8 Å radius to study the influence of the surrounding environment, i.e. hydrophobicity. According to Miyazawa-Jernigan more long-range contacts are obtained by using the centers of side chain atoms (first method), than with either C^{α} atom positions or the centers of all residue atoms including backbone atoms (second method) (Miyazawa and Jernigan, 1985; Manavalan and Ponnuswamy, 1978). However, the PRIFT values of Cornette et al. (Cornette et al., 1987) correlate strongly with both concepts (Table 2). The sense-antisense interaction might be facilitated by the exclusion of water from the pocket in which the receptor binding site is located, as the ligand docks in it (Wolfenden et al., 1979; Brentani, 1988). The fact that contact potentials for hydrophobic amino acids are complemented by contact potentials for hydrophilic residues, and contact potentials for neutral amino acids by those for neutral residues, suggests that an important factor for this type of molecular interaction potential is the minimization of free energy in the peptide—peptide complex (Štambuk et al., 2016a; Kastritis and Bonvin, 2012).

2.3. New tRNA acceptor-stem code and Carter-Wolfenden liphophilic character of amino acids

In 1979, Wolfenden, Cullis and Southgate derived an amino acid scale for free energies in the transfer from the vapor phase to a neutral aqueous solution—closely correlated with the second code letter in the mRNA and DNA (Brentani, 1988). Using this concept, and calculations of amino acid transfers from vapor (v), water (w) and cyclohexane phases (c) Wolfenden et al. (Wolfenden et al., 2015) defined three dimensionless equilibrium constants (K_{eq}): 1. hydrophobicity—for amino acid transfer from aqueous solution at pH 7 to cyclohexane ($K_{w>c}$); 2. hydrophilic character (hydrophilicity)—for amino acid transfer from the vapor phase to aqueous solution at pH 7, at infinite dilution ($K_{v>w}$); and 3. liphophilic character (liphophilicity)—for transfer from the vapor phase to cyclohexane, at infinite dilution ($K_{v>c}$). The transfer equilibrium constants and free energies ($\Delta G = -\,RT\ln K_{eq}$) can be considered to measure the principal forces stabilizing protein structures (Carter and Wolfenden, 2015).

Wolfenden et al. (Wolfenden et al., 2015) showed that the values $\log_{10}(K_{w>c})$, $\log_{10}(K_{v>w})$, and $\log_{10}(K_{v>c})$ represent the basis for hydrophobicity, hydrophilicity and liphophilicity scales, respectively. Multiplication of $K_{w>c}$ by $K_{v>w}$ yields $K_{v>c}$ (Wolfenden et al., 2015), and consequently $\log_{10}(K_{w>c})$ and $\log_{10}(K_{v>w})$ exhibit a strong negative correlation ($r = -0.94$). Their results, which can be found in Table S1 of Ref. (Wolfenden et al., 2015):

$$\log_{10}(K_{v>c}) = \log_{10}(K_{w>c}) + \log_{10}(K_{v>w}) \quad (1)$$

are consistent with the findings of El Tayar et al. (van de Waterbeemd et al., 1994; El Tayar et al., 1995):

$$\text{Lipophilicity} = \text{Hydrophobicity} + \text{Polarity(Hydrophilicity)} \quad (2)$$

We obtained a simple and accurate model of the relationship between hydrophobicity ($\log_{10}(K_{w>c})$) and hydrophilicity ($\log_{10}(K_{v>w})$) corrected for the amino acid mass using the M5 classifer—which combines a rule-based system with a multiple linear regression (Eq. (3), $r = 0.99$, relative absolute error = 9.97%; Weka software, version 3.6.13) (Štambuk et al., 2016a; Witten et al., 2011):

$$\log_{10}(K_{w>c}) = 0.0492 \times \text{mass}_{aa} - 1.0399 \times \log_{10}(K_{v>w}) - 3.1524 \quad (3)$$

The water-to-cyclohexane (w > c) amino acid scale measures the hydrophobicity of the residue, i.e. amino acid's tendency to leave water and enter a nonpolar condensed phase. In a similar way to the "hydrophilic character", the hydrophobicity of the amino acid exhibits: 1. a strong correlation with standard amino acid hydropathy scales (Fig. 2**A**), and 2. a close relationship to the second nucleotide base of mRNA anticodons (Carter and Wolfenden, 2015).

The dependence of hydrophobicity ($\log_{10}(K_{w>c})$) on the hydrophobic moment (PRIFT), hydrophilicity ($\log_{10}(K_{v>w})$) and liphophilicity ($\log_{10}(K_{v>c})$) was also analyzed using the M5 classifer and multiple linear regression (Eq. (4)). The model is very accurate with the correlation coefficient of $r \cong 1$, and relative absolute error of 0.0735%:

$$\log_{10}(K_{w>c}) = 0.0017 \times \text{PRIFT} - 0.9997 \times \log_{10}(K_{v>w}) + 0.9978 \times \log_{10}(K_{v>c}) - 0.0004 \quad (4)$$

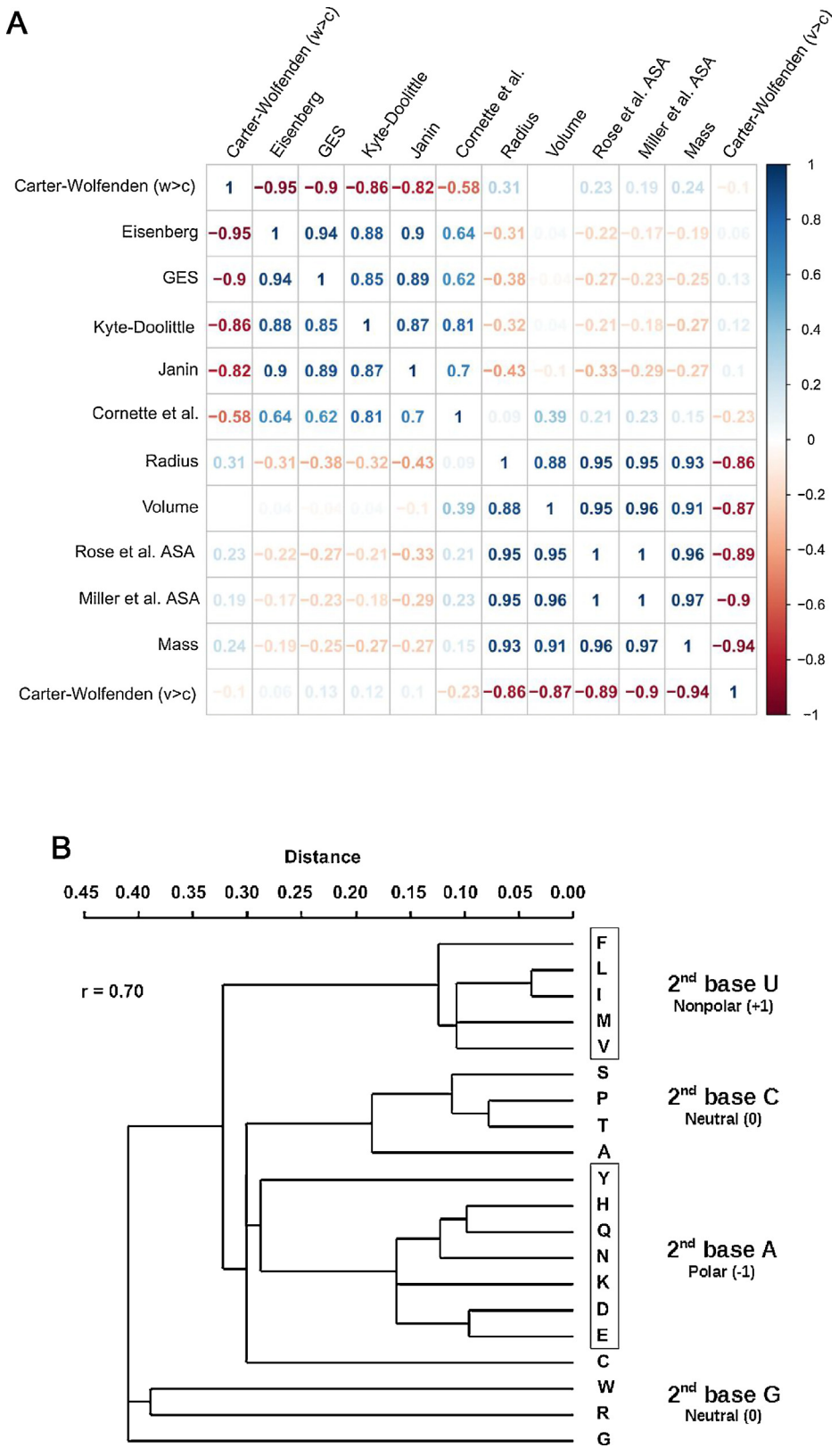

Fig. 2. (**A**) Correlation matrix of 12 amino acid scales representing two main amino acid physico-chemical properties: hydrophobicity (Carter-Wolfenden $G_{w>c}$ (Carter and Wolfenden, 2015), Eisenberg (Eisenberg et al., 1984), GES (Engelman et al., 1986), Kyte-Doolittle (Kyte and Doolittle, 1982), Janin (Janin, 1979), Cornette et al. PRIFT (Cornette et al., 1987)) and lipophilicity/asccessible surface area (Carter-Wolfenden $G_{v>c}$ (Carter and Wolfenden, 2015), Mass (Carter and Wolfenden, 2015), Miller et al. ASA (Miller et al., 1987), Rose et al. ASA (Rose et al., 1985), Volume (Grantham, 1974), Radius (Cootes et al., 1998)). (**B**) Clustering of amino acid scales used in Fig. 2A follows the amino acid distribution associated with the second base column of the genetic code table (Table 1A). Paired-group-algorithm-constrained, Gower similarity index (PAST software, version 3.16). Amino acid (codon) scoring according to Davis (Davis, 1986): hydrophobic amino acid (2^{nd} U) = +1, hydrophilic amino acid (2^{nd} A) = −1, neutral/intermediate amino acid (2^{nd} C and G) = 0.

Table 2
Correlations of PRIFT, Myazawa-Jernigan and Manavalan-Ponnuswamy methods.

Pearson correlation (r)	PRIFT	M-J_A	M-J_B	M-J_C	M-J_D	M-P
PRIFT	1.00	−0.91	−0.93	−0.92	−0.92	0.91
M-J_A	−0.91	1.00	0.96	0.96	0.95	−0.92
M-J_B	−0.93	0.96	1.00	0.99	0.98	−0.92
M-J_C	−0.92	0.96	0.99	1.00	0.99	−0.91
M-J_D	−0.92	0.95	0.98	0.99	1.00	−0.91
M-P	0.91	−0.92	−0.92	−0.91	−0.91	1.00

M-J = Myazawa-Jernigan scale A, B, C and D (Miyazawa and Jernigan, 1999).
M-P = Manavalan-Ponnuswamy scale (Manavalan and Ponnuswamy, 1978).

In 2015 Carter and Wolfenden discovered that the tRNA acceptor-stem code is related to the amino acid liphophilic character of free energies in the transfer from vapor-to-cyclohexane ($G_{v>c}$) (Carter and Wolfenden, 2015). They also confirmed that lipophilic code was distinct from the one allocated in the mRNA anticodon, which is based on the amino acid hydrophobic character free energies of transfer from water-to-cyclohexane ($G_{w>c}$) (Fig. 3**B**).

Carter and Wolfenden first developed an amino acid scale based on the measurement of vapor-to-cyclohexane transfer equilibria ($K_{v>c}$) and free energy determination ($G_{v>c} = \Delta G_{v>c}$, Fig. 3**A** and **C**) (Carter and Wolfenden, 2015; Štambuk et al., 2016b). Secondly, they showed that:

1. the tRNA acceptor-stem code is related to the free energy vapor-to-cyclohexane scale that measures lipophilic character of amino acids ($G_{v>c}$), and
2. lipophilic character of the residue is closely related to the amino acid's size or its solvent-accessible surface area—ASA (Fig. 2**A**) (Carter and Wolfenden, 2015; Štambuk et al., 2016b).

Consequently, the lipophilicity of the residues, measured by vapor-to-cyclohexane free energie values (v > c) shows a strong negative correlation with several amino acid physico-chemical properties: mass, accessible surface area—ASA and size, but no correlation with the hydrophobicity scales (Fig. 2**A**):

a. for Carter and Wolfenden ($G_{v>c}$) vs amino acid mass, r = −0.94;
b. for Carter and Wolfenden ($G_{v>c}$) vs amino acid ASA, r = −0.90;
c. for Carter and Wolfenden ($G_{v>c}$) vs amino acid volume, r = −0.87;
d. for Carter and Wolfenden ($G_{v>c}$) vs amino acid radius, r = −0.86.

Both clusters of amino acid scales from Fig. 2**A** closely follow the amino acid distribution associated with the second base column of the genetic code table (Table 1A and Fig. 2**B**). The same grouping could be obtained using individual clusters (hydrophobicity r = 0.52, lipophilicity/ASA r = 0.62), but the correlation coefficient is better when both scale clusters are used (r = 0.70). Additionally, Fig. 3**D** shows that hydrophobicity ($G_{w>c}$) and lipophilicity ($G_{v>c}$), together with the parameters of mass and weighted average surface accessibilities (folded ASAs) are closely related to the process of selection of amino acids by corresponding class I and class II aminoacyl-tRNA synthetases, as discussed by Carter and Wolfenden in Ref. (Carter and Wolfenden, 2015)—Table S1.

Fig. 4**A** and **B** show that the free energies ($G_{v>c}$) of the Carter-Wolfenden vapor-to-cyclohexane (v > c) lipophilic scale are strongly correlated with the complementary coding of sense—antisense peptide interactions in both translation directions. The result implies that the novel tRNA acceptor-stem code defines complementary peptide interaction (or pairing) in a manner different from standard hydrophobicity and hydrophilic character patterns. This difference is defined by an alternative tRNA coding pattern based on the lipophilic character of the residues, closely related to molecule size or accessible surface area—ASA (Carter and Wolfenden, 2015; Štambuk et al., 2016b; Tien et al., 2013).

Vapor-to-cyclohexane transfer equilibria measure the van der Waals forces that attract a solute from the vapor phase to the walls of a nonpolar solvent cavity minus the cost of making that cavity (Carter and Wolfenden, 2015; Štambuk et al., 2016b). ASA represents the area over which the center of a water molecule retains van der Waals contacts with the amino acid side-chain in a Gly-X-Gly tripeptide, without penetrating other atoms (Carter and Wolfenden, 2015; Štambuk et al., 2016b). The solvent-accessible surface area–ASA, maximum possible solvent-accessible surface area for the residue (MaxASA) and relative accessible surface area, i.e. relative solvent accessibility (RSA = ASA/MaxASA), are often used as a measure of residue solvent exposure (Tien et al., 2013; Ahmad et al., 2003).

The results presented in Table 1, Figs. 1 and 4 show that hydrophilic and hydrophobic amino acids form a cluster of amino acids defined by means of the complementary second codon bases A and U, respectively. Another amino acid cluster consists of predominately neutral amino acids specified by the complementary second codon bases G and C (Table 1, Figs. 1 and 4). The clustering model presented in Figs. 1 and 4 is comfirmed by partitioning around medoids (PAM; R software version 3.4.2, manhattan-metric-standardized) (Štambuk and Konjevoda, 2003; Spector, 2011)—using physicochemical scales of Fig. 2**A** vs Davis scores of polarity according to the second codon position (Fig. 2**B**).

2.4. *tRNA acceptor-stem coding related to 2nd codon base*

For the vapor-to-cyclohexane amino acid lipophilic scale the following is valid:

1. the scale is not correlated with the hydropathy scales presented in Fig. 2A ($-0.23 \leq r \leq 0.13$);
2. it was derived by a different measurement procedure, i.e. by the calculation of free energy values in vapor-to-cyclohexane environments ($G_{v>c}$), rather than in water-to-cyclohexane environments ($G_{w>c}$);
3. its clustering of complementary amino acid pairs is identical to the clustering observed for the hydrophobic moment consensus scale—PRIFT (Table 1B, Figs. 1 and 4).

Additionally, as shown in Table 3, Figs. A1 and A2, this common type of amino acid free-energy-based pairing within two extracted cluster types (polar-nonpolar, neutral-neutral) is strongly dependent on the central/second *purine base* of the mRNA codon (i.e. tRNA anticodon) irrespective of:

1. the lipophilic character or hydrophobic character of the residues, and
2. the direction of translation.

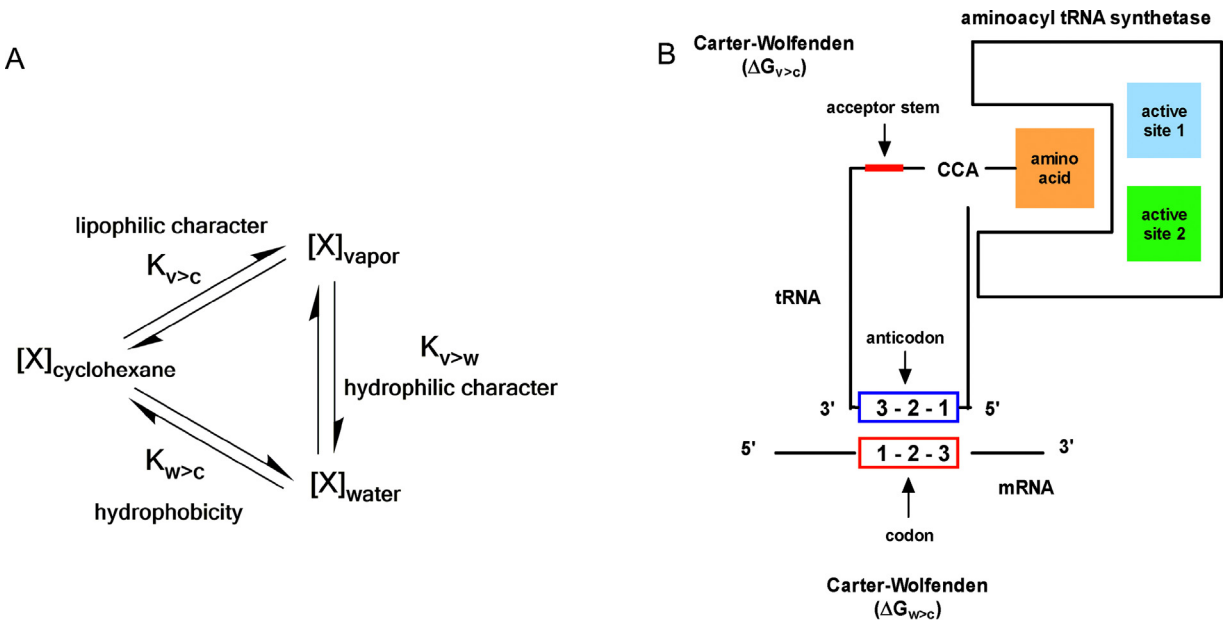

C

2nd base	Amino Acid [1]	Carter-Wolfenden ($\Delta G_{w>c}$) [2]	Carter-Wolfenden ($\Delta G_{v>c}$) [3]
U	Phenylalanine (F)	-3.60	-4.36
	Leucine (L)	-5.79	-3.51
	Isoleucine (I)	-5.79	-3.64
	Methionine (M)	-2.61	-4.09
	Valine (V)	-5.58	-3.59
C	Serine (S)	3.85	-1.95
	Proline (P)	-5.12	-2.14
	Threonine (T)	1.90	-2.47
	Alanine (A)	-2.89	-0.94
A	Tyrosine (Y)	0.42	-5.69
	Histidine (H)	5.17	-5.10
	Glutamine (Q)	5.55	-3.83
	Asparagine (N)	6.66	-3.02
	Lysine (K)	6.26	-3.26
	Aspartic acid (D)	7.55	-3.40
	Glutamic acid (E)	8.06	-4.18
G	Cysteine (C)	-2.09	-3.33
	Tryptophane (W)	-2.50	-8.38
	Arginine (R)	14.90	-5.02
	Glycine (G)	-0.27	2.12

[1] aaRS: class I, class I/II, class II

[2] w>c = water-to-cyclohexane

[3] v>c = vapor-to-cyclohexane

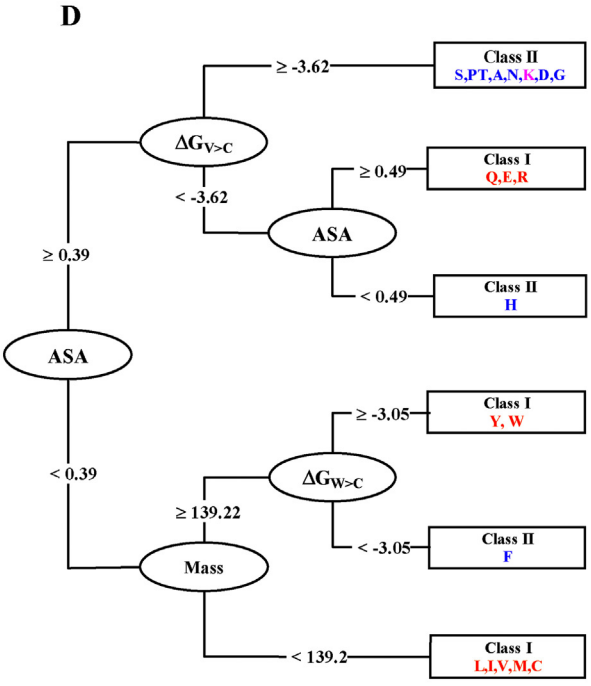

Fig. 3. (**A**) Equilibrium constants (K_{eq}) of amino acid transfer from vapor (v), water (w) and cyclohexane phases (c) (**B**) Lipophilic t-RNA acceptor-stem code according to the Carter-Wolfenden model ($G_{v>c} = \Delta G_{v>c}$), which is distinct from a hydrophobic code allocated in the mRNA anticodon ($G_{w>c} = \Delta G_{w>c}$). (**C**) Carter-Wolfenden water-to-cyclohexane ($G_{w>c} = \Delta G_{w>c}$) and vapor-to-cyclohexane ($G_{v>c} = \Delta G_{v>c}$) transfer equilibria and free energy determination related to the aminoacyl-tRNA synthetase-(aaRS)-based selection of the residues. (**D**) The relationship between four different amino acid physicochemical properties in Ref. (Carter and Wolfenden, 2015)—Table S1 and corresponding class I and class II aminoacyl-tRNA synthetases was analyzed using Random Tree classifier (Weka software, version 3.6.13 (Witten et al., 2011)).

Table 3 clearly shows that the central/second *pyrimidine base* of the mRNA codon is not significantly correlated with the amino acid pairing based on the hydrophobicity and lipophilicity values of the clusters examined.

One plausibile interpretation of this phenomenon related to *purine—pyrimidine* coding of the sense—antisense peptide interactions could be that the 2nd *purine* of the codon defines amino acids that tend to be exposed due to the combined effects of residue contact potentials ("hydrophobic character") and their accessible surface areas ("lipophilic character"). Consequently, in addition to the proposed tRNA acceptor-stem code for amino acid size and asccessible surface area there seems to exist one more checking algorithm, confirming Carter-Wolfenden "lipophilic" model, at the level of the 2nd *purine—pyrimidine* base interaction of the *complementary mRNA codon—tRNA anticodon complexes*.

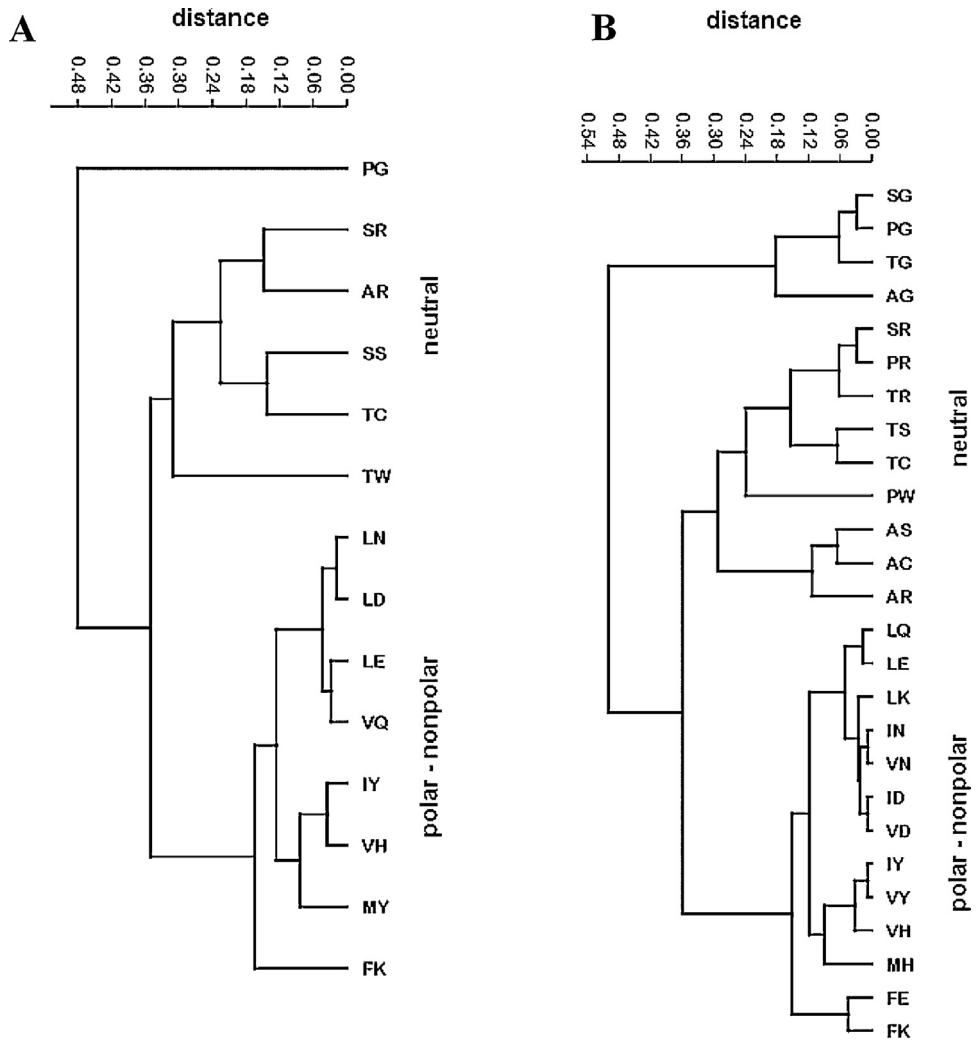

Fig. 4. Lipophilicity values of the complementary amino acid pairs (Carter-Wolfenden vapor-to-cyclohexane, Table 1B) form two distinct clusters composed of polar-nonpolar and neutral residues. (**A**) Complementary (sense – antisense) pairs of the genetic code translated in 3′ → 5′ direction, r = 0.85; (**B**) Complementary (sense – antisense) pairs of the genetic code translated in 5′ → 3′ direction, r = 0.84. Paired group algorithm, Gower similarity index (PAST software, version 3.16).

Table 3
Correlation of complementary amino acid (aa) pairs in 3′ → 5′ and 5′ → 3′ translation direction with respect to amino acid hydrophobicity and lipophilicity. x = ligand$_{aa}$ = amino acid hydrophobicity or lipophilicity (2nd base *purine* or *pyrimidine*), y = |ligand$_{aa}$ – receptor$_{aa}$| = absolute difference in amino acid hydrophobicity or lipophilicity (2nd base *purine* or *pyrimidine*).

Complementary aa pairs (translation direction)	polar-nonpolar (3′ → 5′)	neutral-neutral (3′ → 5′)	polar-nonpolar (5′ → 3′)	neutral-neutral (5′ → 3′)
2nd purine base				
Hydrophobicity[a]	**0.98***	**0.87***	**0.98***	**0.81***
Lipophilicity[b]	**0.96***	**0.99***	**0.95***	**0.98***
2nd pyrimidine base				
Hydrophobicity[a]	0.56	0.64	0.50	0.56
Lipophilicity[b]	0.22	0.17	0.30	0.13

[a] Cornette et al. (PRIFT) (Cornette et al., 1987).
[b] Carter-Wolfenden free energy ($G_{v>c}$) (Carter and Wolfenden, 2015).
* $p < 0.05$ (Pearson r).

Hydrophilic amino acids are coded by the second purine base of the codon (Table 1A, Fig. 2**B**). Considering distribution and complementarity of hydropathy in multi-subunit proteins, i.e. at a higher structural level, Korn and Burnett found that "subunits that bind predominantly through hydrophilic forces, such as hydrogen bonds, ionic pairs, and water and metal bridges, are involved in dynamic quaternary organization and allostery" (Korn and Burnett, 1991).

Euclidean amino acid pair distances, $d_{ij} = \sqrt{(\Delta G_{w>cij}/\sigma G_{w>c})^2 + (\Delta G_{v>cij}/\sigma G_{v>c})^2}$, of both Carter-Wolfenden water-to-cyclohexane and vapor-to-cyclohexane scales were calculated by Štambuk et al. (Štambuk et al., 2016b). $\Delta G_{w>cij}$ are amino acid free energies from water-to-cyclohexane (w > c), and $\Delta G_{v>cij}$ are amino acid free energies from vapor-to-cyclohexane (v > c). $\sigma G_{w>c}$ and $\sigma G_{v>c}$ are standard deviations of $\Delta G_{w>cij}$ and $\Delta G_{v>cij}$, respectively. These distances, based on Carter-Wolfenden hydrophobicity and lipophilicity parameters, exhibit significant correlation with the Miyata distances (Miyata et al., 1979) derived in 1979 using amino acid hydropathies and volumes (r = 0.71) and reconstruct the columns of the genetic code

table, thus confirming the Carter-Wolfenden method (Carter and Wolfenden, 2015).

It remains an open question if such distances could be used as a supplement to PAM and BLOSUM matrices in an analysis of closely-related protein sequences (Štambuk et al., 2016b). It could also be used in QSAR studies to quantify the substitution of one or more amino acid within a peptide chain (Štambuk et al., 2016b). The procedure takes into account the difference between the embedding of the amino acid's physico-chemical properties into the tRNA acceptor-stem and mRNA bases. The genetic code is translated by the aminoacyl-tRNA synthetases and their cognate transfer RNAs. Related bi-directional coding, i.e. middle-base pairing in the synthetase antisense alignments, represents an important unification of the proteome—consistent with sense-antisense coding (Chandrasekaran et al., 2013; Carter, 2017).

The results imply that the flow of information from nucleic acids to proteins, with related sense—antisense peptide interaction phenomena, is more complex than the situation described by the hydrophobicity concept of the genetic code (Root-Bernstein, 2015; Biro, 2007). Recent developments in this field could enable the development of new algorithms for the analysis of the structure, function and evolution of protein and nucleotide sequences (Root-Bernstein, 2015; Carter and Wolfenden, 2015; Štambuk and Konjevoda, 2017a; Wolfenden et al., 2015; Štambuk et al., 2016b). The prediction of protein—protein interactions and rational design of peptide ligands will also benefit from new insights into the genetic coding of complementary peptides.

2.5. Practical applications of sense-antisense peptide modeling

In the following text we will address several practical applications of sense-antisense peptide modeling illustrated with different interaction assay types based on: microscale thermophoresis (MST), tryptophan fluorescence spectroscopy (TFS), nuclear magnetic resonance spectroscopy (NMR), and magnetic particles enzyme immunoassay (MPEIA).

Four different ligand-acceptor binding events under varying circumstances are considered as examples.

1. In the first example microscale thermophoresis was successfully employed to analyze the binding of $ACTH_{1-10}$ and its short antisense peptide ligand $LVKAT_{5-9}$.
2. The second ligand binding assay used tryptophan fluorescence spectroscopy to evaluate how L- and D-enantiomers of Met-enkephalin bound L-antisense peptide IPPKY.
3. The third target was a CD20 epitope$_{168-181}$. Low affinity binding to the antisense paratope was analyzed efficiently with NMR spectroscopy.
4. Finally, as the fourth example, magnetic particles enzyme immunoassay was used to model the binding of erythropoietin epitopes P4 and P5 to their antisense paratopes.

2.5.1. Microscale thermophoresis (MST)—binding of $ACTH_{1-10}$ and its short antisense$_{5-9}$

Microscale thermophoresis represents a fast and accurate assay for the study of peptide–peptide interactions (Jerabek-Willemsen et al., 2011; Wienken et al., 2010; Turčić et al., 2015). We used it to analyse the binding of $ACTH_{1-10}$ to its antisense peptide $LVKAT_{5-9}$ targeting ACTH pharmacophore region $HFRV_{6-9}$ (3'→5' translation according to Root-Bernstein (Root-Bernstein, 2015; Houra et al., 2011; Root-Bernstein and Holsworth, 1998)).

Microscale thermophoresis observed the binding event between peptidic fragments $ACTH_{1-10}$ and a $LVKAT_{5-9}$ antisense titrant (GenScript, Piscataway, NJ, USA). The interaction seen on Fig. 5 shows a single binding event in the micromolar concentration range of the titrant. In the MST-experiment we have

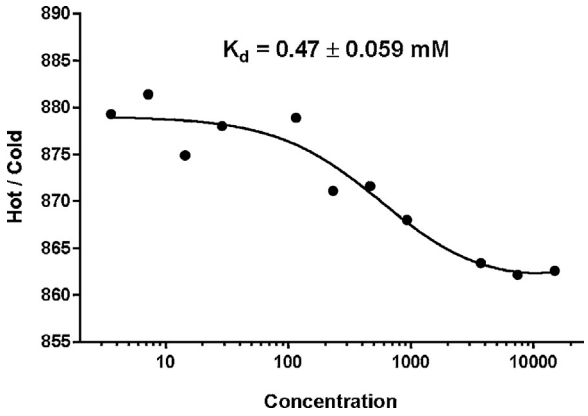

Fig. 5. The binding of $ACTH_{1-10}$ and its antisense peptide ($LVKAT_{5-9}$) observed with microscale thermophoresis.

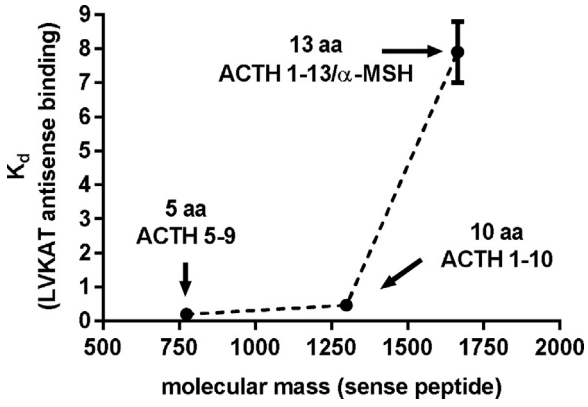

Fig. 6. The binding of $ACTH_{5-9}$, $ACTH_{1-10}$ and $ACTH_{1-13}$ to the short antisense peptide $LVKAT_{5-9}$ targeting the ACTH pharmacophore region $HFRW_{6-9}$.

kept the concentration of the $ACTH_{1-10}$ Trp-containing fragment constant, while the concentration of the non-fluorescent binding partner ($LVKAT_{5-9}$) was varied between 60 mM and 1.8311 μM. After a short period of incubation the samples were loaded into MST NT.LabelFree standard glass capillaries and the MST-analysis was performed using the Monolith.NT.LabelFree (NanoTemper Technologies GmbH, Munich, Germany). The experimental data show consequent titrant ($LVKAT_{5-9}$) concentration dependency of $ACTH_{1-10}$ fragment interaction. The results give an efficient fit with a K_d of 465 μM (SE = 59.4 μM).

The tryptophan fluorescence studies of LVKAT antisense binding to different ACTH fragments is shown in Fig. 6. It is clearly visable that the constant of dissociation (K_d) rises from 0.2 ± 0.02 mM for $ACTH_{5-9}$ and 0.47 ± 0.02 mM for $ACTH_{1-10}$ to 7.9 ± 0.9 mM for $ACTH_{1-13}$ (Houra et al., 2011), i.e. the affinity for LVKAT binding drops with the rise in ACTH chain length. The results also suggest that shorter peptides lacking significant secondary and tertiary conformation are preferable in modeling bioactive parts of larger polypeptides and proteins (Root-Bernstein, 2015) (see also Fig. 10). Additionally, as emphasized by Tropsha et al. (Tropsha et al., 1992): "The composition of the antisense peptide is more important than the conformation imposed by the sequence determining the affinity of small sense and antisense peptides".

2.5.2. Fluorescence spectroscopy—binding of Met-enkephalin enantiomers and L-antisense

Met-enkephalin is an endogenous opioid pentapeptide (YGGFM) with biological effects on neurotransmission and neuroimmunomodulation, and strong protective effects in differ-

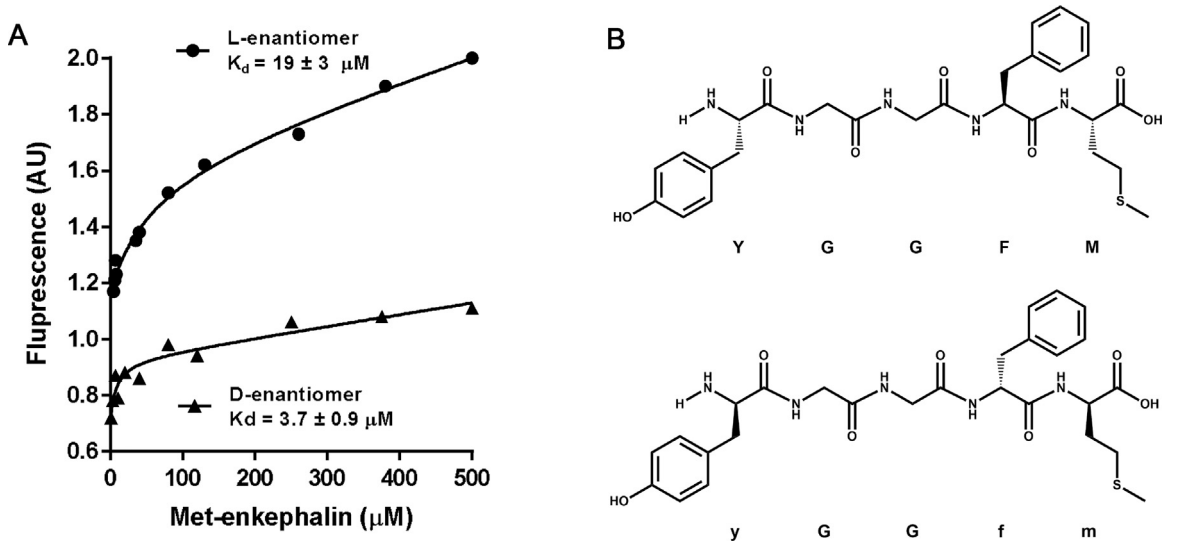

Fig. 7. (**A**) The binding of L- and D-Met enkephalin to the antisense peptide L-IPPKY was detected using tryptophan fluorescence spectroscopy. (**B**) Primary structures of L- and D-Met enkephalin enantiomers. L- amino acid and glycine are denoted using capital letters, and D-amino acids with small letters. L-Met-enkephalin (LUPEX®, Biofactor GmbH, Bad Harzburg, Germany), D-Met enkephalin and L-IPPKY (GenScript, Piscataway, NJ, USA).

ent animal disease models (Martinić et al., 2014). Natural peptides are made of L-amino acids, while D-amino acids are rarely found (Turčić et al., 2009).

The binding of L-Met-enkephalin and its antisense peptide L-IPPKY was detected by fluorescence spectroscopy ($K_d = 19 \pm 3\ \mu M$) (Martinić et al., 2014). The biological assay showed that when Met-enkephalin was preincubated with antisense peptide, its protective effects were lost, in line with the fluorescence spectroscopy study (Martinić et al., 2014). Due to achiral glycine–glycine dipeptide, at the central part of the molecule, L- and D-Met-enkephalin enantiomers seem to have similar spatial positions of the amino acid functional groups at positions 1 (Y) and 4–5 (F–M), both rotated with respect to the glycine–glycine (G–G) part at positions 2 and 3 (Fig. 7**B**). Therefore we investigated the binding of L- and D-Met-enkephalin to the L-IPPKY antisense (3′→5′ translation).

Fluorescence spectra were measured by OLIS RSM 1000F spectrofluorimeter (Bogart, Georgia, USA) equipped with thermostated cell at 25 °C (Martinić et al., 2014). The excitation wavelength was set at 290 nm in order to diminish the fluorescence of phenylalanine and maximize the fluorescence of tryptophan (Martinić et al., 2014). In our titrations, both species exhibited fluorescence (e.g. D-YGGFM or L-YGGFM, and L-IPPKYW) but the phenylalanine present in D-YGGFM or L-YGGFM, which was in excess, had a much smaller quantum yield than the tryptophan present in L-IPPKYW.

Data obtained from the titrations were analyzed with Specfit® software and three spectrally active species were suggested by single value decomposition (SVD) analysis. Both reactants are fluorophores and the third spectrally active species was attributed to the complex of two reactants. Analysis also suggested 1:1 complex formation and did not indicate any higher order complexes in either case. Consequently, the model proposed is that given by Eq. (5) where K_d is the dissociation constant of the complex (Eq. (6)):

$$\mathrm{L-IPPKYW-L(D)-YGGFM} \rightleftarrows \mathrm{L-IPPKYW + L(D)-YGGFM} \quad (5)$$

$$\mathrm{Kd} = \frac{[\mathrm{L-IPPKYW}][\mathrm{L(D)-YGGFM}]}{[\mathrm{L-IPPKYW-L(D)YGGFM}]} \quad (6)$$

The dissociation constants (mean ± SD) calculated from the fluorescence titrations for complexes of L-YGGFM and D-YGGFM with L-IPPKYW are $19 \pm 3\ \mu M$ and $3.7 \pm 0.9\ \mu M$, respectively (Fig. 7**A**). These results indicate a slightly stronger affinity of D-YGGFM for L-IPPKYW, although both of dissociation constants are within a similar range of micromolar values. As shown by Martinić, D-Met-enkephalin exhibits hepatoprotective results similar to L-Met-enkephalin in the murine experimental hepatitis model (Martinić, 2014). These protective effects could be eliminated by L-IPPKY antisense (Martinić, 2014), according to the fluorescence spectroscopy study (Fig. 7**A**). Our data suggest that antisense technology is applicable to D-forms (Root-Bernstein, 2007).

2.5.3. NMR spectroscopy—low affinity binding of CD20 epitope$_{168\text{-}181}$ and antisense paratope

The CD20 antigen is an important biomarker for diagnosis and therapy of non-Hodgkin lymphoma (Binder et al., 2006; Klein et al., 2013). Rituximab is a monoclonal antibody to CD 20, widely used in the treatment of malignant lymphoma and autoimmune diseases (Klein et al., 2013). Binder et al. (Binder et al., 2006; Klein et al., 2013) showed that CD20 extracellular loop 142–188 posseses two rituximab binding domains, i.e. rituximab binds a discontinuous epitope in CD20, comprised of $ANPS_{170–173}$ and $YCYSI_{182–185}$.

Using 3′→5′ translation rule we derived an antisense peptide to the region 168–181 EPANPSEKNSPSTQ (Fig. 8). This region had been predicted by several methods to be antigenic and exposed (Kyte-Doolittle, PRIFT, RVP-net (Kyte and Doolittle, 1982; Štambuk and Konjevoda, 2017a; Ahmad et al., 2003)). The sequence $EPANPSEKNSPSTQ_{168–181}$ was translated in the 3′→5′ complement direction and the antisense peptide LGRLGSLFLSGSWV was selected by BLAST search, as a combination of the most probable antisense (antibody) fragments within the sliding block of 5 residues (Štambuk et al., 2014). By joining fragments LGRLG, GSLFL and SGSWV we obtained a final linear antisense sequence LGRLGSLFLSGSWV, consisting of three human antibody fragments (Fig. 8**A**).

Fig. 9 presents the binding interaction between bioactive fragment of the human CD20 peptide, $EPANPSEKNSPSTQ_{168–181}$, and its antisense peptide LGRLGSLFLSGSWV (GenScript, Piscataway, NJ, USA). NMR spectroscopy could provide useful information regarding sense-antisense peptide complexes (Tropsha et al., 1992). The study has been done using 500 MHz ^{1}H NMR titrations. Spectra were recorded on a Bruker Avance II 500 spectrometer. The addition of increasing amounts of the antisense peptide LGRLGSLFLSGSWV caused chemical shift changes for several protons in the peptide EPANPSEKNSPSTQ. Two of the proton resonances of the human CD 20 peptide EPANPSEKNSPSTQ which moved

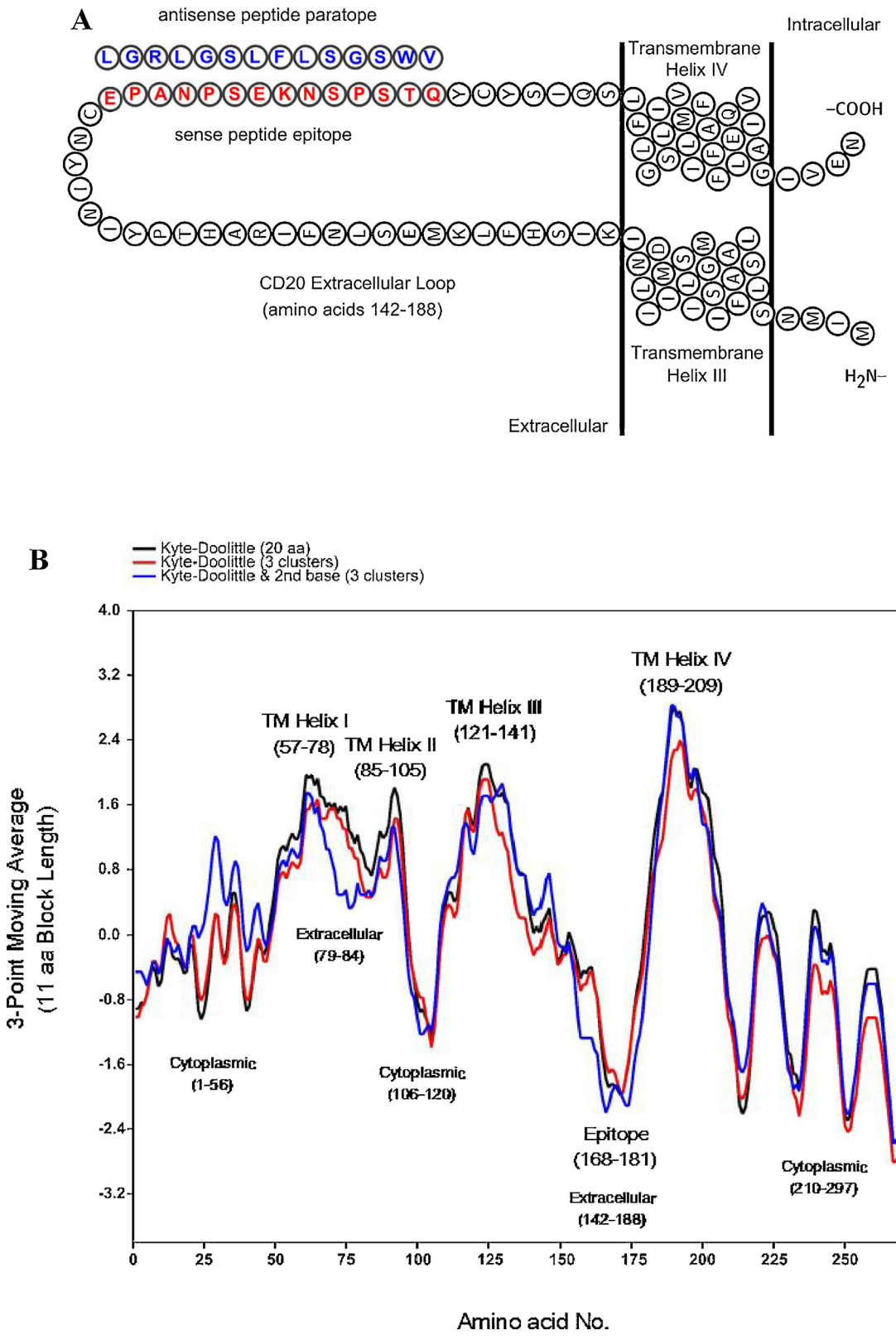

Fig. 8. (**A**) Human CD20 epitope EPANPSEKNSPSTQ$_{168\text{-}181}$ and its antisense peptide LGRLGSLFLSGSWV (in 3′ → 5′ direction). (**B**) Detection of CD20 epitope and transmenmbrane (TM) helices using the Kyte-Doolittle scale based on: 1. twenty amino acids (black) (Kyte and Doolittle, 1982), 2. average values of three clusters of amino acids (red) (Kyte and Doolittle, 1982), and 3. three medoids (blue) calculated using partition around medoids for Kyte-Doolittle values and hydropathy score of the 2nd codon position in Fig. 2B (nonpolar aa cluster: L, V, I, F, M—medoid L = 3.8; neutral aa cluster: T,G, S, W, P, A, C, R—medoid S = −0.8; polar aa cluster: Q, N, D, E, H, K, Y—medoid E = −3.5; manhattan-metric-standardized, silhouette width = 0.74, R software version 3.4.2). Pearson correlation between three used variables is in the range from 0.95 to 0.99.

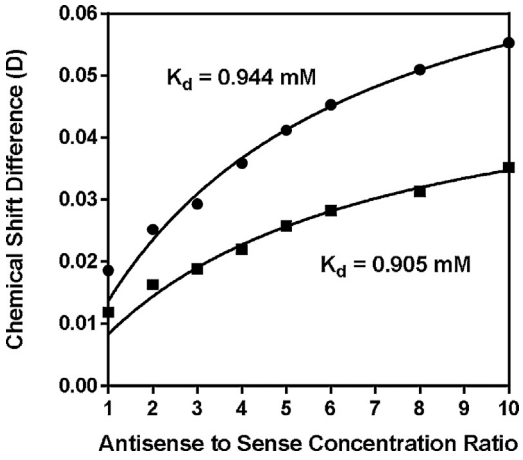

Fig. 9. Binding study using ^{1}H NMR chemical shift titration of antisense peptide LGRLGSLFLSGSWV and its sense CD20 peptide EPANPSEKNSPSTQ$_{168\text{-}181}$.

gradually and were evidently in fast exchange throughout the titration were selected as an appropriate marker of the equilibrium conditions. The titration protocol was designed so that the concentration of EPANPSEKNSPSTQ remained constant at 0.27 mM, as the concentration of antisense LGRLGSLFLSGSWV was subjected to incremental increases: 0.27, 0.54, 0.81, 1.08, 1.35, 1.62, 2.16, 2.7 mM (Scheme B1, Appendix B).

The non-linear least-squares fitting of the observed ^{1}H chemical shifts to the equation (7) shown below yielded the equilibrium dissociation constant, K_d:

$$\Delta_{obs} = 0.5\Delta_{max}\{1 + X + K_d/[P]_0 - [(1 + X + /K_d/[P]_0)^2 - 4X]^{1/2}\} (7)$$

where X is the molar ratio of the two peptides and [P]0 was set to 0.27 mM (see above and Scheme B1—Appendix B). K_d and Δ_{max} were fitted (Fielding, 2007). The dissociation constants of the complex were 0.944 mM and 0.905 mM, respectively (Fig. 9). The result indicated low affinity binding of the CD20 peptide epitope EPANPSEKNSPSTQ$_{168\text{–}181}$ and its 3′ → 5′ antisense paratope LGRLGSLFLSGSWV. The results of NMR experiments confirm that this method can detect low affinity interactions, difficult to determine with other methods (Musselman and Kutateladze, 2016).

The data obtained support the concept that NMR is a useful method for determining low-affinity binding $K_d > 10$ μM. However, with $K_d < 10$ μM, alternative methods (fluorescence spectroscopy and microscale thermophoresis) are better because the high protein concentrations needed in NMR measurements will lead to stoichiometric binding conditions (Musselman and Kutateladze, 2016). The data imply that NMR spectroscopy and 3′ → 5′ translation modeling of antisense peptides could be used to model the low affinity binding of ligand–acceptor, i.e. epitope–paratope, motifs.

2.5.4. Magnetic particles enzyme immunoassay (MPEIA)—binding of erythropoietin to antisense paratopes P4 and P5

Erythropoietin (EPO) is the primary humoral regulator of red blood cell production (Fibi et al., 1991). It has five well-characterized regions, P1-P5, suitable for the investigation of potential binding sites (Štambuk et al., 2014; Štambuk et al., 2016a; Fibi et al., 1991). We recently designed an EPO antisense peptide DFDIWPLRTAWPLS, by the 3′ → 5′ translation of its P2 carboxyl-terminal domain LKLYTGEACRTGDR$_{153\text{-}166}$ (Štambuk et al., 2014). When coated to magnetic nanoparticles P2 antisense captures EPO, at its receptor binding site 153–166, which enables its quantification with the magnetic particles enzyme immunoassay (MPEIA), either using an antibody or a biotinylated antisense peptide to P4 region (aa 9–22, SRVLERYLLEAKEA) (Štambuk et al., 2016a). The P4 antisense peptide RAQDLSIDELRFLR-Lys (Biotin) was equally successful in detecting Erythropoietin-alpha, and Darbepoetin alfa modified with two additional sialic acid-containing carbohydrate chains (aa 30 and 88), even in the low concentration range (Štambuk et al., 2016a).

In this study we compared the detections of Erythropoietin-alpha and Darbepoetin alfa by two distant secondary antisense motifs—P4 at aa 9–22 and P5 at aa 112–123 (CASLO, Lyngby, Denmark). P5 region LGAQKEAISPPD$_{112\text{-}123}$ was translated in the 3′ → 5′ direction to obtain antisense peptide DPRVFLRYSGGL-Lys(Biotin). Primary antisense motif DFDIWPLRTAWPLS of the carboxyl-terminal P2 domain was used to capture Erythropoietin-alpha, and Darbepoetin alfa to magnetic nanoparticles.

2.5.5. Coating of carboxyl magnetic particles with peptides

SPHERO™ carboxyl magnetic particles (1.0–1.4 μm) were coated with either test peptide (antisense peptide DFDIWPLRTAWPLS directed to the selected EPO-α region P2—aa 153–166, Fig. 10**A**–**C**) (Štambuk et al., 2014; Štambuk et al., 2016a; Spherotech Inc., 2017) or the control (erythropoietin unrelated peptide YGGFM, Fig. 10**D**) using the one step 1-ethyl-3-(3-dimethylaminopropyl) carbodiimide (EDC) coupling method as suggested by manufacturer.

Briefly, reaction mixtures were composed of a 2 mL sodium acetate buffer (0.01 M, pH 5.0), 1 mg of peptide, 0.2 mL of 2.5% w/v carboxyl magnetic particles, 10 mg of EDC. Reactions proceeded in glass reaction tubes for two hours at room temperature with occasional vortexing. Tubes were centrifuged at 3000*g* for 15 min, the supernatant was carefully discarded, and the pellets were twice washed in 4 mL of isotonic buffered saline (IBS), followed by centrifugation. After washing, magnetic particles were re-suspended in IBS to obtain a 0.125% w/v suspension.

2.5.6. Comparison of magnetic particle enzyme immunoassay with detection by biotinylated peptide

Four fold serial dilutions (from 1000 ng to 0.98 ng) of two commercial preparations of erythropoietin (recombinant human erythropoietin-alpha—rHuEPO-α, ProSpec, East Brunswick, NJ, USA and Darbepoetin alfa—Aranesp®, Amgen Europe B.V., Breda, NL) were made in 96-well microtiter plates to generate standard curves. A suspension (0.125% w/v) of carboxyl magnetic particles, coated with either test or control peptide was added (25 μL/well). The plates were incubated at room temperature for 30 min and washed with PBS-Tween three times. The washing solution was removed each time by using the Spherotech UltraMag Separator.

For the magnetic particle assay using biotinylated antisense peptides, 100 μL of the peptides RAQDLSIDELRFLR-Lys(Biotin) or DPRVFLRYSGGL-Lys(Biotin) in PBS (125 ng/μL) was added to the wells and incubated at room temperature for 30 min. The plates were washed and 100 μL of anti-biotin-peroxidase antibody produced in goats (Sigma-Aldrich, St. Louis, MO, USA) diluted in PBS (1:2000) was added to the wells. The plate was placed in an incubator for 30 min at room temperature, washed and SIGMA*FAST*™ OPD peroxidase substrate was added to the wells. After 30 min incubation in the dark, the reaction was stopped with 3 M HCl and the absorbances read at 492 nm.

The results presented in Fig. 10 shows that antisense peptides targeting P4 and P5 regions of the native and glycosylated derivatives of erythropoietin could be successfully applied for their quantification, instead of antibodies. Two component bispecific (Bs) assay with simultaneous detection of biotinylated antisense peptides to Darbepoetin alfa (Aranesp®) regions P4 and P5 in Fig. 10**C** exhibited almost identical standard curves according to the individual P4 and P5 Darbepoetin alfa (Aranesp®) measurements presented in Fig. 10**B**. This indicates that specific antisense peptides targeting EPO regions P4 and P5 did not cross-react, either mutually or with other binding region (Fig. 10**C**). In a similar way to

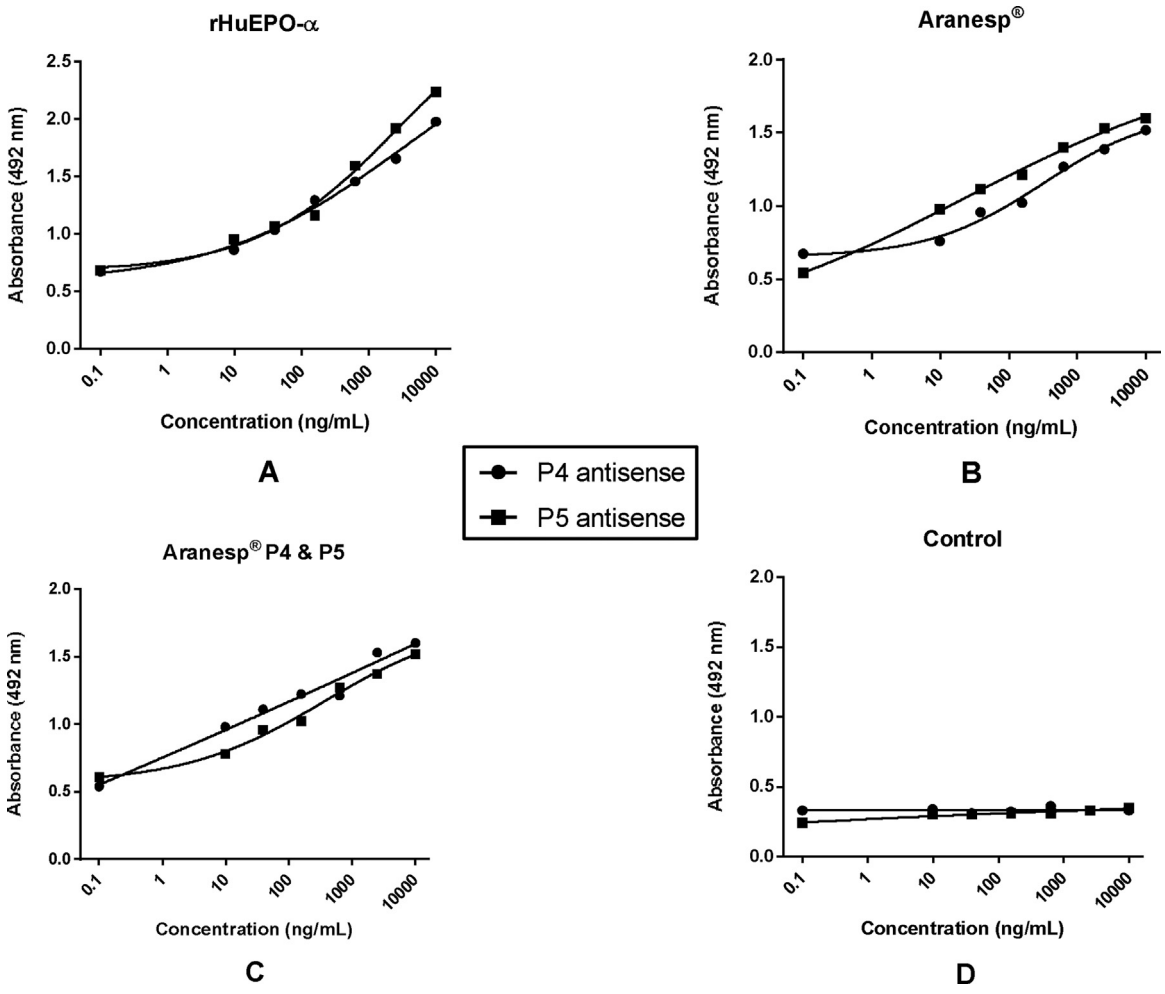

Fig. 10. (**A**) Detection of recombinant human erythropoietin-alpha (rHuEPO-α) by Magnetic Particle Ezyme Immunoassay (MPEIA), using biotinylated antisense peptides to regions P4 (RAQDLSIDELRFLR$_{9-22}$) and P5 (DPRVFLRYSGGLK$_{112-123}$). (**B**) Detection of Darbepoetin alfa (Aranesp®) by Magnetic Particle Ezyme Immunoassay (MPEIA), using biotinylated antisense peptides to regions P4 (RAQDLSIDELRFLR$_{9-22}$) and P5 (DPRVFLRYSGGLK$_{112-123}$). (**C**) Detection of Darbepoetin alfa (Aranesp®) by Magnetic Particle Ezyme Immunoassay (MPEIA), using two component (bispecific) assay with biotinylated antisense peptides to regions P4 (RAQDLSIDELRFLR$_{9-22}$) and P5 (DPRVFLRYSGGLK$_{112-123}$). (**D**) Magnetic Particle Ezyme Immunoassay (MPEIA) failure to detect the binding of Darbepoetin alfa (Aranesp®) or recombinant human erythropoietin-alpha (rHuEPO-α) when unrelated peptide (Met-enkephalin — YGGFM) was coupled to SPHERO™ carboxyl magnetic particles instead of EPO capturing P2 antisense—DFDIWPLRTAWPLS.

the situation with bispecific antibodies (BsAb) (Fan et al., 2015), this dual specificity of protein antisense paratopes (BsAp) could open up a wide range of possibilities for biomedical applications.

The concept of sense–antisense peptide binding and design may also be used for the separation of molecules and cells from different body fluids, e.g., using SEPMAG technology and immunopurification (Štambuk et al., 2016a; Sepmag Systems, 2017).

3. Conclusions

1. Antisense peptides bind to each other with high affinity. Important factors for such binding are the number of available sense—antisense peptide structures arising from the bidirectional transcription and translation of RNA sequences, and physicochemical properties of amino acids encoded by the genetic code table. The interplay of both factors influences the specificity of the ligand–receptor interactions, and affects the selection and evolution of such peptide ligand–receptor systems.
2. The nucleotide information specified by the *complementary mRNA codon—tRNA anticodon complexes*, and recently discovered *tRNA acceptor-stem code* provide the basis for the rational modeling of sense—antisense peptide interactions.
3. The genetic coding algorithm for sense and antisense peptide interactions is based on hydrophobic and lipophilic amino acid physico-chemical properties, i.e. the tendency of residues to leave water/vapor and enter a nonpolar condensed phase—dependent on the parameters of mass, size and accessible surface area.

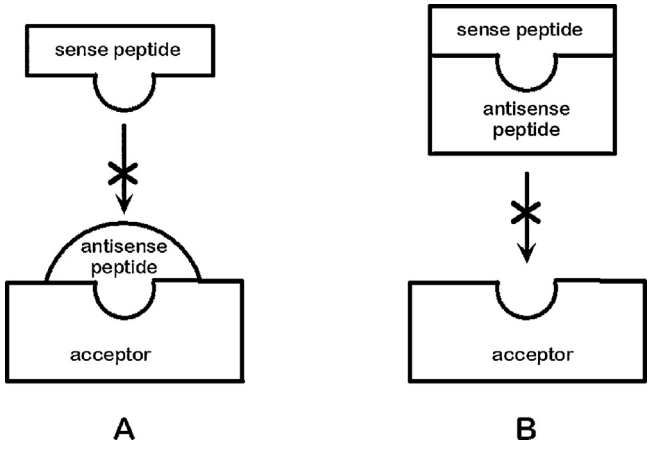

Fig. 11. Modulation of acceptor (**A**) and sense peptide (**B**) using complementary, i.e. antisense, peptides.

4. The interaction and clustering of complementary amino acid pairs according to hydrophobic and lipophilic free-energy values is strongly dependent on the central (second) *purine base* of the mRNA codon and its *pyrimidine* complement of the tRNA anticodon.
5. Antisense peptides can be used to derive bioactive peptide fragments, and to modulate the activity of acceptors and ligands (Fig. 11). Different interaction assays based on microscale thermophoresis (MST), tryptophan fluorescence spectroscopy (TFS), nuclear magnetic resonance spectroscopy (NMR) and magnetic particle enzyme immunoassay (MPEIA) enable quick and accurate screening of the potentially bioactive antisense peptides with optimal activity. Selected antisense peptides are potential lead compounds for the development of novel diagnostic, prognostic and therapeutic substances, biopharmaceuticals and vaccines.

Author contributions

N.Š. and P.K. wrote the paper and carried out the theoretical investigation, modeling and design, while the experimental investigation and the description of methods were carried out by M.G. (fluorescence spectroscopy, NMR), P.T. (fluorescence spectroscopy, MST), K.K. (NMR spectroscopy), R.N-K. and Z.M. (magnetic nanoparticle immunoassay).

Conflicts of interest

The authors declare no conflict of interest.

Acknowledgments

This work was supported by the Croatian Ministry of Science, Education and Sports (grant No. 098-0982929-2524) and the Croatian Institute for Toxicology and Anti-doping. The authors thank Dr. Piotr Wardega for his assistance in the microscale thermophoresis experiment.

Appendix A

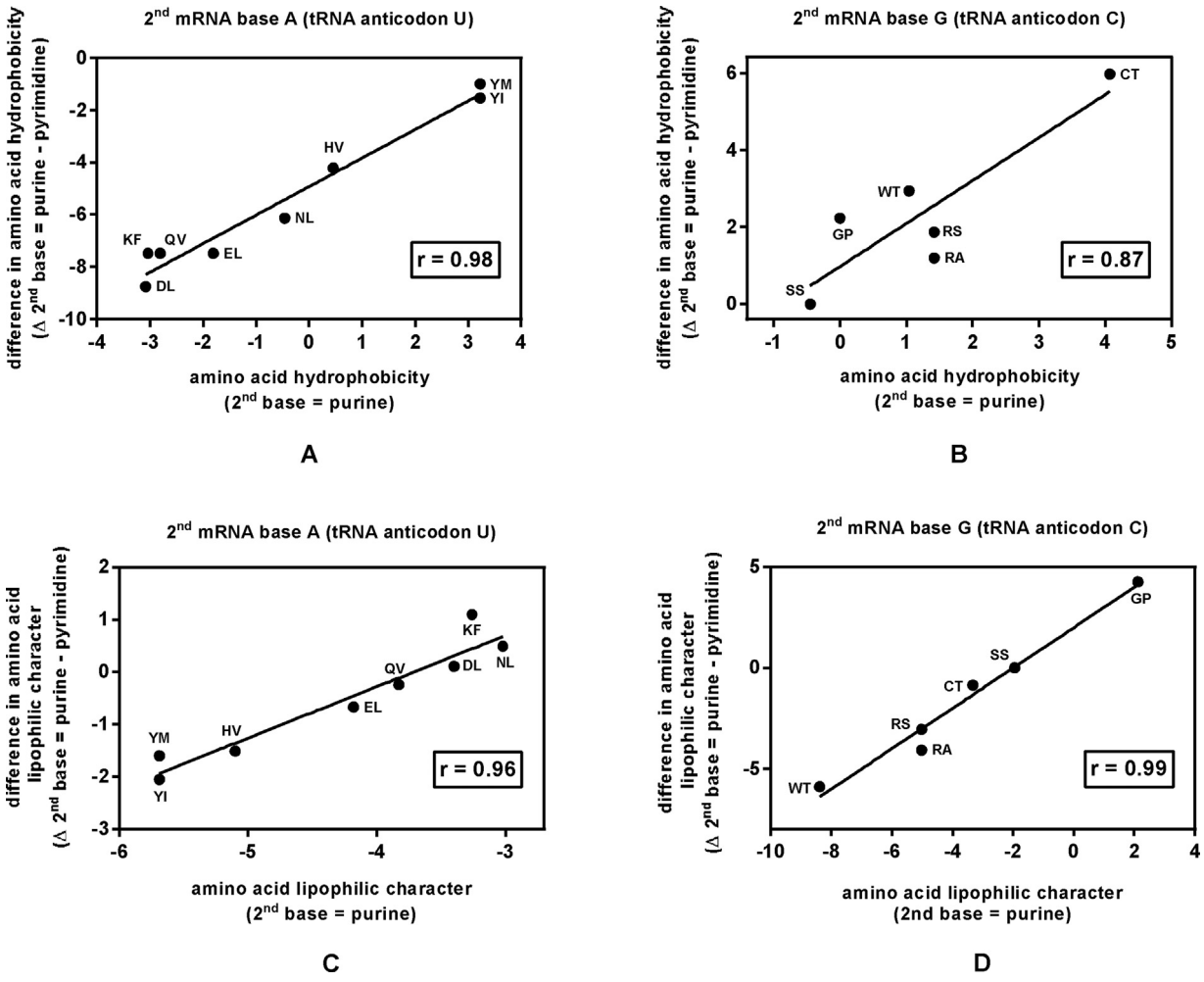

Fig. A1. (**A**) Correlation of complementary pairs of *polar residues* in 3′ → 5′ translation direction with respect to amino acid hydrophobicity (aa, PRIFT scale (Cornette et al., 1987)); (**B**) Correlation of complementary pairs of *neutral residues* in 3′ → 5′ translation direction with respect to amino acid hydrophobicity (aa, PRIFT scale (Cornette et al., 1987)); (**C**) Correlation of complementary pairs of *polar residues* in 3′ → 5′ translation direction with respect to amino acid liphophilicity (aa, Carter-Wolfenden vapor-to-cyclohexane scale—$G_{v>c}$ (Carter and Wolfenden, 2015)); (**D**) Correlation of complementary pairs of *neutral residues* in 3′ → 5′ translation direction with respect to amino acid liphophilicity (aa, Carter-Wolfenden vapor-to-cyclohexane scale—$G_{v>c}$ (Carter and Wolfenden, 2015)). x = free energy $ligand_{aa}$, y = $|ligand_{aa} - receptor_{aa}|$ free energy absolute difference; r value represents Pearson correlation.

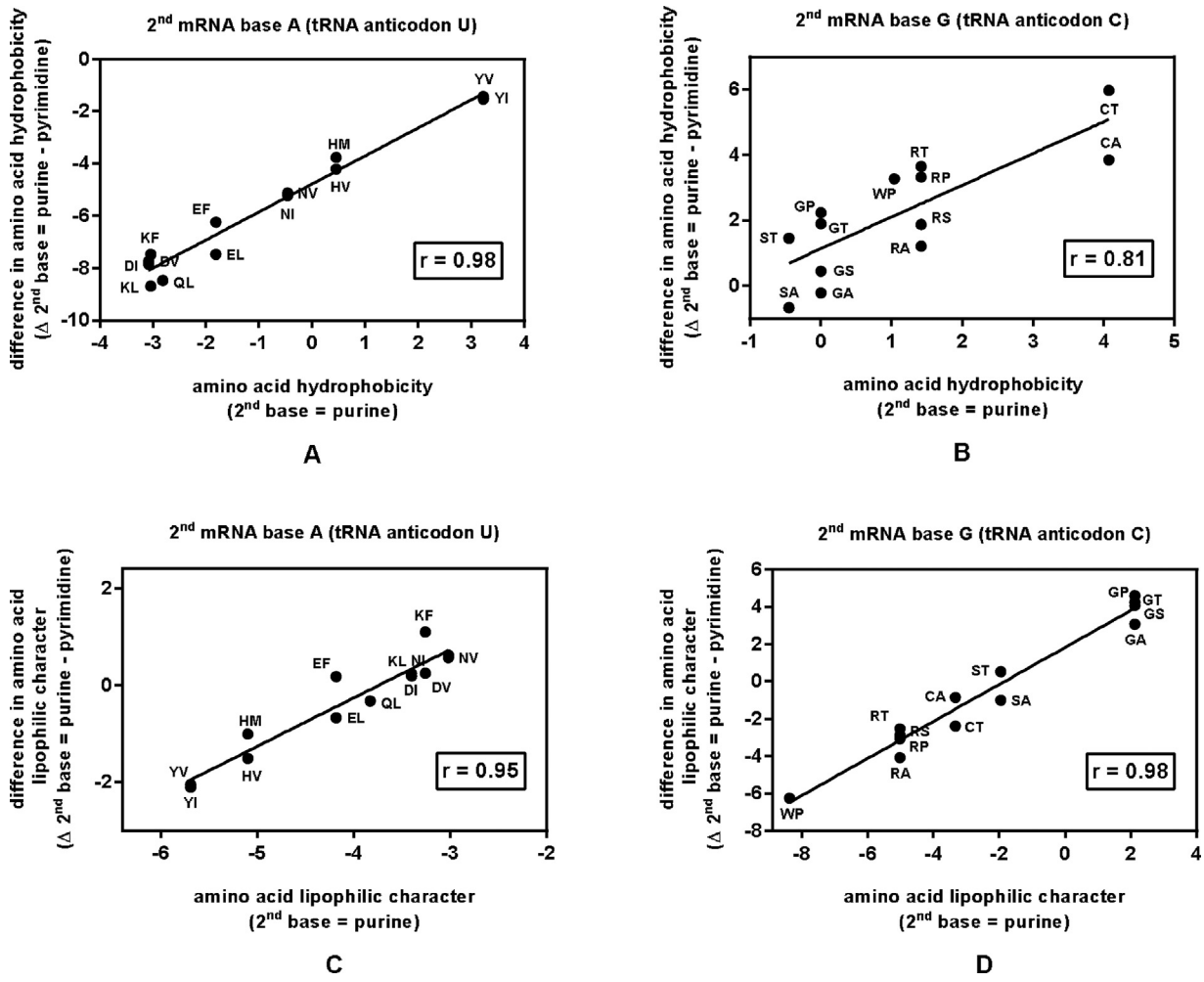

Fig. A2. (**A**) Correlation of complementary pairs of *polar residues* in 5′ → 3′ translation direction with respect to amino acid hydrophobicity (aa, PRIFT scale (Cornette et al., 1987)); (**B**) Correlation of complementary pairs of *neutral residues* in 5′ → 3′ translation direction with respect to amino acid hydrophobicity (aa, PRIFT scale (Cornette et al., 1987)); (**C**) Correlation of complementary pairs of *polar residues* in 5′ → 3′ translation direction with respect to amino acid liphophilicity (aa, Carter-Wolfenden vapor-to-cyclohexane scale—$G_{v>c}$ (Carter and Wolfenden, 2015)); (**D**) Correlation of complementary pairs of *neutral residues* in 5′ → 3′ translation direction with respect to amino acid liphophilicity (aa, Carter-Wolfenden vapor-to-cyclohexane scale—$G_{v>c}$ (Carter and Wolfenden, 2015)). x = free energy $ligand_{aa}$, y = |$ligand_{aa}$ – $receptor_{aa}$| free energy absolute difference; r value represents Pearson correlation.

Appendix B

Chemical shift changes (in ppm) monitored for one of the proton resonances of sense peptide EPANPSEKNSPSTQ (human CD20 aa 168-181) upon titration with antisense peptide LGRLGSLFLSGSWV (Figure 9, ●)

```
>> D1
D1 =
   0.0186
   0.0252
   0.0293
   0.0359
   0.0412
   0.0453
   0.0510
   0.0553
```

Chemical shift changes (in ppm) monitored for another proton resonance of sense peptide EPANPSEKNSPSTQ upon titration with its antisense peptide LGRLGSLFLSGSWV (Figure 9, ■)

```
>> D3
D3 =
   0.0119
   0.0163
   0.0189
   0.0220
   0.0258
   0.0283
   0.0314
   0.0352
```

Concentration of antisense peptide LGRLGSLFLSGSWV (in mM)

```
>> L0
L0 =
   0.2700
   0.5400
   0.8100
   1.0800
   1.3500
   1.6200
   2.1600
   2.7000
```

Constant concentration of sense peptide EPANPSEKNSPSTQ (in mM)

```
>> P0
P0 = 0.2700
```

Scheme B1. ^{1}H NMR chemical shift titration study (500 MHz, T = 300 K, peptides dissolved in 500 ul H_2O/D_2O = 9:1, spectra were recorded on a Bruker Avance II 500 spectrometer).

References

Ahmad, S., Gromiha, M.M., Sarai, A., 2003. RVP-net: online prediction of real valued accessible surface area of proteins from single sequences. Bioinformatics 19, 1849–1851.

Binder, M., Otto, F., Mertelsmann, R., Veelken, H., Trepel, M., 2006. The epitope recognized by rituximab. Blood 15, 1975–1978.

Biro, J.C., 2007. The proteomic code: a molecular recognition code for proteins. Theor. Biol. Med. Model. 4, 45.

Blalock, J.E., Bost, K.L., 1986. Binding of peptides that are specified by complementary RNAs. Biochem. J. 234, 679–683.

Blalock, J.E., 1995. Genetic origin of protein shape and interaction rules. Nat. Med. 1, 876–878.

Brentani, R.R., 1988. Biological implications of complementary hydropathy of amino acids. J. Theor. Biol. 135, 495–499.

Carter, C.W., Wolfenden, R., 2015. tRNA acceptor stem and anticodon bases form independent codes related to protein folding. Proc. Natl. Acad. Sci. U. S. A. 112, 7484–7488.

Carter, C.W., Wolfenden, R., 2016. tRNA acceptor-stem and anticodon bases embed separate features of amino acid chemistry. RNA Biol. 13, 145–151.

Carter, C.W., 2017. 2017. Coding of class I and II aminoacyl-tRNA synthetases. Adv. Exp. Med. Biol., 1–46, http://dx.doi.org/10.1007/5584_2017_93.

Chandrasekaran, S.N., Yardimci, G.G., Erdogan, O., Roach, J., Carter, C.W., 2013. Statistical evaluation of the Rodin-Ohno hypothesis: sense/antisense coding of ancestral class I and II aminoacyl-tRNA synthetases. Mol. Biol. Evol. 30, 1588–1604.

Cootes, A.P., Curmi, P.M.G., Cunningham, R., Donnelly, C., Torda, A.E., 1998. The dependence of amino acid pair correlations on structural environment. Protein. Struct. Funct. Genet. 32, 175–189.

Cornette, J.L., Cease, K.B., Margalit, H., Spouge, J.L., Berzofsky, J.A., DeLisi, C., 1987. Hydrophobicity scales and computational techniques for detecting amphipathic structures in proteins. J. Mol. Biol. 195, 659–685.

Davis, L.C., 1986. Simple scoring method finds membrane-spanning peptides. Biochem. Educ. 14, 186–189.

Eisenberg, D., Weiss, R.M., Terwilliger, T.C., 1984. The hydrophobic moment detects periodicity in protein hydrophobicity. Proc. Natl. Acad. Sci. U. S. A. 81, 140–144.

El Tayar, N., Karajiannis, H., van de Waterbeemd, H., 1995. Structure-lipophilicity relationships of peptides and peptidomimetics. Amino Acids 8, 125–139.

Engelman, D.M., Steitz, T.A., Goldman, A., 1986. Identifying nonpolar transbilayer helices in amino acid sequences of membrane proteins. Annu. Rev. Biophys. Biophys. Chem. 15, 321–353.

Fan, G., Wang, Z., Hao, M., Li, J., 2015. Bispecific antibodies and their applications. J. Hematol. Oncol. 8, 130.

Fibi, M.R., Stüber, W., Hintz-Obertreis, P., Lüben, G., Krumwieh, D., Siebold, B., Zettlmeissl, G., Küpper, H.A., 1991. Evidence for the location of the receptor-binding site of human erythropoietin at the carboxyl-terminal domain. Blood 77, 1203–1210.

Fielding, L., 2007. NMR methods for the determination of protein-ligand dissociation constants. Prog. Nucl. Magn. Reson. Spectrosc. 51, 219–242.

Grantham, R., 1974. Amino acid difference formula to help explain protein evolution. Science 185, 862–864.

Houra, K., Turčić, P., Gabričević, M., Weitner, T., Konjevoda, P., Štambuk, N., 2011. Interaction of α-melanocortin and its pentapeptide antisense LVKAT: effects on hepatoprotection in male CBA mice. Molecules 16, 7331–7343.

Janin, J., 1979. Surface and inside volumes in globular proteins. Nature 277, 491–492.

Jerabek-Willemsen, M., Wienken, C.J., Braun, D., Baaske, P., Duhr, S., 2011. Molecular interaction studies using microscale thermophoresis. Assay Drug. Dev. Technol. 9, 342–353.

Kastritis, P.L., Bonvin, A.M.J.J., 2012. On the binding affinity of macromolecular interactions: daring to ask why proteins interact. Interface 10, e1–5e27.

Klein, C., Lammens, A., Schäfer, W., Georges, G., Schwaiger, M., Mössner, E., Hopfner, K.P., Umana, P., Niederfellner, G., 2013. Epitope interactions of monoclonal antibodies targeting CD20 and their relationship to functional properties. MAbs 5, 22–33.

Korn, A.P., Burnett, R.M., 1991. Distribution and complementarity of hydropathy in multisubunit proteins. Protein Struct. Funct. Genet. 9, 37–55.

Kyte, J., Doolittle, R.F., 1982. A simple method for displaying the hydropathic character of a protein. J. Mol. Biol. 157, 105–132.

Le, S., Worch, T., 2014. Analyzing Sensory Data with R. CRC Press, Boca Ratton.

Manavalan, P., Ponnuswamy, P.K., 1978. Hydrophobic character of amino acid residues in globular proteins. Nature 275, 673–674.

Martinić, R., Šošić, H., Turčić, P., Konjevoda, P., Fučić, A., Stojković, R., Aralica, G., Gabričević, M., Weitner, T., Štambuk, N., 2014. Hepatoprotective effects of met-enkephalin on acetaminophen-induced liver lesions in male CBA mice. Molecules 19, 11833–11845.

Martinić, R., 2014. Biological Effects of D-Met-Enkephalin Isomer in a Murine Model of Chemical Liver Injury Induced by Paracetamol. Ph.D. Thesis. Faculty of Science, University of Zagreb, Zagreb, Croatia, pp. 1–94.

Mekler, L.B., Idlis, R.G., 1981. Construction of models of three-dimensional biological polypeptide and nucleoprotein molecules in agreement with a general code which determines specific linear recognition and binding of amino acid residues of polypeptides to each other and to the trinucleotides of polynucleotides [in Russian]. In: Deposited Doc. VINITI, pp. 1476–1481.

Mekler, L.B., 1970. Specific selective interaction between amino acid residues of the polypeptide chains. Biophys. USSR 14, 613–617.

Mihel, J., Šikić, M., Tomić, S., Jeren, B., Vlahović, K., 2008. PSAIA – protein structure and interaction analyzer. BMC Struct. Biol. 8, 21.

Miller, S., Janin, J., Lesk, A.M., Chothia, C., 1987. Interior and surface of monomeric proteins. J. Mol. Biol. 196, 641–656.

Miller, A.D., 2015. Sense-antisense (complementary) peptide interactions and the proteomic code; potential opportunities in biology and pharmaceutical science. Expert Opin. Biol. Ther. 15, 245–267.

Miyata, T., Miyazawa, S., Yasunaga, T., 1979. Two types of amino acid substitutions in protein evolution. J. Mol. Evol. 12, 219–236.

Miyazawa, S., Jernigan, R.L., 1985. Estimation of effective interresidue contact energies from protein crystal structures: quasi-chemical approximation. Macromolecules 18, 534–552.

Miyazawa, S., Jernigan, R.L., 1999. Self-consistent estimation of inter-residue protein contact energies based on an equilibrium mixture approximation of eesidues. Proteins 34, 49–68.

Musselman, C.A., Kutateladze, T.G., 2016. Preparation, biochemical analysis, and structure determination of methyllysine readers. In: Pyle, A.M., Christianson, D.W. (Eds.), Methods in Enzymology 573: Enzymes of Epigenetics, Part A. Academic Press, Cambridge, pp. 345–362.

Root-Bernstein, R.S., Holsworth, D.D., 1998. Antisense peptides: a critical mini-review. J. Theor. Biol. 190, 107–119.

Root-Bernstein, R.S., 1982. Amino acid pairing. J. Theor. Biol. 94, 885–894.

Root-Bernstein, R.S., 2005. Peptide self-aggregation and peptide complementarity as bases for the evolution of peptide receptors: a review. J. Mol. Recognit. 18, 40–49.

Root-Bernstein, R., 2007. Simultaneous origin of homochirality, the genetic code and its directionality. Bioessays 29, 689–698.

Root-Bernstein, R., 2015. How to make a non-antigenic protein (auto) antigenic: molecular complementarity alters antigen processing and activates adaptive-innate immunity synergy. Anticancer Agents Med. Chem. 15, 1242–1259.

Rose, G.D., Geselowitz, A.R., Lesser, G.J., Lee, R.H., Zehfus, M.H., 1985. Hydrophobicity of amino acid residues in globular proteins. Science 229, 834–838.

Sepmag Systems, 2017. The Basic Guide to Magnetic Bead Cell Separation, http://www.sepmag.eu/free-basic-guide-magnetic-bead-cell-separation (Accessed 7 July 17).

Siemion, I.Z., Cebrat, M., Kluczyk, A., 2004. The problem of amino acid complementarity and antisense peptides. Curr. Protein Pept. Sci. 5, 507–527.

Spector, P., 2011. Concepts in Computing with Data. Cluster Analysis, https://www.stat.berkeley.edu/?s133/Cluster2a.html (Accessed 18 September 2017).

Spherotech Inc, 2017. SpheroTechnical Notes #10 – Magnetic Particle Enzyme Immunoassay (MPEIA) Test Procedure. Spherotech Inc, http://www.spherotech.com/tech_SpheroTech_Note_10.html (Accessed 7 July 17).

Štambuk, N., Konjevoda, P., 2003. Prediction of secondary protein structure with binary coding patterns of amino acid and nucleotide physicochemical properties. Int. J. Quant. Chem. 92, 123–134.

Štambuk, N., Konjevoda, P., 2016. The genetic coding algorithm for complementary peptide interaction. Symmetry: Cult. Sci. 27, 155–161.

Štambuk, N., Konjevoda, P., 2017a. Structural and functional modeling of artificial bioactive proteins. Information 8, E1–E29.

Štambuk, N., Konjevoda, P., 2017b. The hydrophobic moment: an early bioinformatics method and de novo protein design. Science http://science.sciencemag.org/content/355/6321/201/tab-e-letters (Accessed 7 July 17).

Štambuk, N., Manojlović, Z., Turčić, P., Martinić, R., Konjevoda, P., Weitner, T., Wardega, P., Gabričević, M., 2014. A simple three-step method for design and affinity testing of new antisense peptides: an example of erythropoietin. Int. J. Mol. Sci. 15, 9209–9223.

Štambuk, N., Konjevoda, P., Manojlović, Z., Novak Kujundžić, R., 2016a. The use of the Miyazawa-Jernigan residue contact potential in analyses of molecular interaction and recognition with complementary peptides. In: Ortuno, F., Rojas, I. (Eds.), Bioinformatics and Biomedical Engineering, 9656. IWBBIO, LNBI, pp. 91–102.

Štambuk, N., Konjevoda, P., Manojlović, Z., 2016b. Miyazawa-Jernigan contact potentials and Carter-Wolfenden vapor-to-cyclohexane and water-to-cyclohexane scales as parameters for calculating amino acid pair distances. In: Ortuno, F., Rojas, I. (Eds.), Bioinformatics and Biomedical Engineering, 9656. IWBBIO 2016, LNBI, pp. 358–365.

Tien, M.Z., Meyer, A.G., Sydykova, D.K., Spielman, S.J., Wilke, C.O., 2013. Maximum allowed solvent accessibilites of residues in proteins. PLoS One 8, e80635.

Tropsha, A., Kizert, J.S., Chaiken, I.M., 1992. Making sense from antisense: a review of experimental aata and developing ideas on sense-antisense peptide recognition. J. Mol. Recognit. 5, 43–54.

Turčić, P., Bradamante, M., Houra, K., Štambuk, N., Kelava, T., Konjevoda, P., Kazazić, S., Vikić-Topić, D., Pokrić, B., 2009. Effects of alpha-melanocortin enantiomers on acetaminophen induced hepatotoxicity in CBA mice. Molecules 14, 5017–5026.

Turčić, P., Štambuk, N., Konjevoda, P., Kelava, T., Gabričević, M., Stojković, R., Aralica, G., 2015. Modulation of γ_2-MSH hepatoprotection by antisense peptides and melanocortin subtype 3 and 4 receptor antagonists. Med. Chem. 11, 286–925.

van de Waterbeemd, H., Karajiannis, H., El Tayar, N., 1994. Lipophilicity of amino acids. Amino Acids 7, 129–145.

Wienken, C.J., Baaske, P., Rothbauer, U., Braun, D., Duhr, S., 2010. Protein-binding assays in biological liquids using microscale thermophoresis. Nat. Commun. 1, 100, http://dx.doi.org/10.1038/ncomms1093.

Witten, I.H., Frank, E., Hall, M.A., 2011. Data Mining: Practical Machine Learning Tools and Techniques. Morgan Kaufmann, Amsterdam.
Wolfenden, R.V., Cullis, P.M., Southgate, C.C.F., 1979. Water, protein folding, and the genetic code. Science 206, 575–577.
Wolfenden, R., Lewis, C.A., Yuan, Y., Carter, C.W., 2015. Temperature dependence of amino acid hydrophobicities. Proc. Natl. Acad. Sci. U. S. A. 112, 7484–7488.
Zull, J.Z., Smith, S.K., 1990. Is genetic code redundancy related to retention of structural information in both DNA strands? Trends Biochem. Sci. 15, 257–261.